uc3m | Universidad Carlos III de Madrid

BACHELOR'S THESIS

Degree in Aerospace Engineering

Atmospheric models evaluation for space applications

Elena Odriozola Olavarría

September 2018

Supervisor
Guillermo Ramos Hernández

Abstract

This Bachelor's Thesis aims to evaluate how well atmospheric models used for space applications, such as orbit determination, represent the upper atmosphere. For this purpose, atmospheric conditions provided by state-of-the-art models are compared to actual satellite measurements.

A detailed description of the atmosphere is given for a better understanding of its dynamic behaviour. Atmospheric modeling complexity is realized, mainly due to the unpredictability of solar activity and the difficulty of its introduction into the models through solar and magnetic indices. Furthermore, insight in the development of semi-empirical and empirical models is given as well as in the inputs they need for their computations.

Further work ideas are realized throughout the development of the project, as well as the positive socioeconomic impact accurate atmospheric modeling can have on the aerospace industry.

KEY WORDS: atmospheric models, atmosphere, solar activity

LaTeX was used as text editor.

Matlab 2017b was used as programming tool.

Images created and/or edited with Microsoft PowerPoint 2016,
Adobe Illustrator CSx, Office and Photoshop CS6.

All referenced Figures are original or searched in Google
under the “Free to use, share or modify” filter.

Acknowledgements

First of all, I would like to thank my tutor Guillermo for helping me write this thesis, specially since it was done over the summer and it is not always easy to stay as focused. I highly appreciate his constant encouragement and positiveness on not-so-well going days.

Secondly, I would like to thank my professors for the three years of their teaching I have received. It has been very nice to find professors who care about their students and encourage them to do their best. I am specially grateful to the university for granting me the opportunity to study abroad in the United States. I can say it was an unforgettable and eye-opening experience I wouldn't have had otherwise, and the friends I have made are priceless.

Thirdly, thank you to all the friends I have made along the way, the ones I have lived with and the ones I have shared most of my time with. Thank you Diego for teaching me all I know about LaTeX , you are the best. Of course I want to mention my friends from home, who keep being by my side year after year, even though we no longer see each other every day. Thank you María for making every minute we spend together the funnest of times, I miss you already. A special shout-out to my best man Manu, for making me laugh like there is no tomorrow with things only him could make up. Who would have thought we would become best friends when I first stalked you in algebra? You are welcome.

Last but not least, I would like to thank my family, specially my parents, Miguel and Ana, for supporting me in every decision I make and for giving me the best life I could ask for. I can't wait to see what's ahead and to share it with you all.

Contents

List of Figures

List of Tables

1 Introduction

1.1 Description of the Problem

On October 4, 1957, the Soviet Union became the first nation to have successfully launched a satellite into Earth's orbit. *Sputnik 1* became the first artificial satellite in history, settling a milestone for humankind and leading out to the *space era* [1]. Since that day, over 6 000 satellites have been launched. Around 3 000 are still in orbit, although a rough estimate of 1 000 are functioning meanwhile the rest of them account for *space debris*, commonly known as *space junk* [2].

Artificial satellites orbiting Earth are used in several different fields, such as space science, Earth observation, meteorology, climate research, telecommunication, navigation and human space exploration, due to them being a unique resource of scientific data. Depending on their purpose, they are strategically placed on different geocentric orbits: Low Earth Orbit (LEO), Medium Earth Orbit (MEO), or the Geosynchronous Orbit (GSO).

As an example of satellite development, the *International Space Station (ISS)* is to be mentioned. The *ISS* is a habitable artificial satellite product of the association between European countries (represented by ESA), The United States (NASA), CANADA (CSA), Japan (JAXA) and Russia (Roscosmos). Since the *ISS* nearly weighs 400 tones, it would have been not possible to launch it all at once; such powerful nor big enough rocket exists. Therefore, the *ISS* has been launched into space (LEO) piece-by-piece, in more than 40 missions, starting in 1998 [3]. As it can be perceived in Figures 1 and 2, the *ISS* has come a long way from the first satellite *Sputnik*.

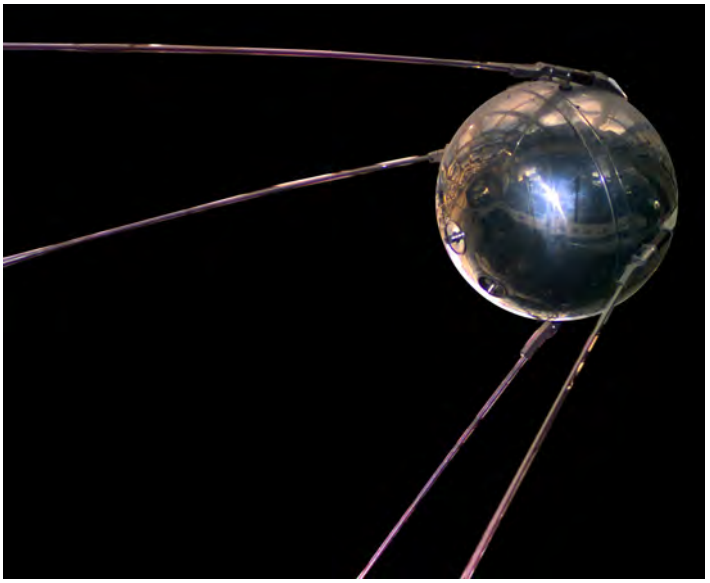

Figure 1: *Sputnik 1* [4]

Figure 2: *International Space Station* [5]

The beginning of manned spacecraft was led out by USSR/Russia's *Vostok 1* in 1961. *Vostok 1* carried the Soviet cosmonaut Yuri Gagarin and reentered the atmosphere after one orbit, one hour and 48 minutes after launch [6]. On the same year and just a few weeks later, the U.S launched its first and the world's second manned spacecraft, *Freedom 7*, which carried the American astronaut Alan Shepard and performed a 15-minute suborbital spaceflight [7].

To appreciate the development of manned spacecraft, NASA's fourth space shuttle *Atlantis OV-104* is to be mentioned. Its construction began in 1980 and it was delivered to the *Kennedy Space Center*, Florida, in 1985. *STS 51-J* on October 3, 1985, was her maiden voyage. It was dedicated to a Department of Defense payload deployment and it lasted four days, one hour and 45 minutes. *Atlantis* completed 33 different missions, carrying up to seven crew members in each one. It served as an on-orbit launch site for spacecraft, like the interplanetary probe *Galileo*. It also delivered components to the *ISS*, like in her last mission on July 8, 2011, *STS-135*. Such mission lasted 13 days, being the U.S 135^{th} space shuttle fight [8]. Overall, *Atlantis* spent 306 days, 14 hours and 12 minutes in space, orbited Earth 4 848 times and travelled 202 673 974 kilometers [9]. This is quite an achievement, considering that 24 years before, *Sputnik 1* just orbited once around Earth. See Figures 3, 4 and 5 for a visual glimpse of manned spacecraft development.

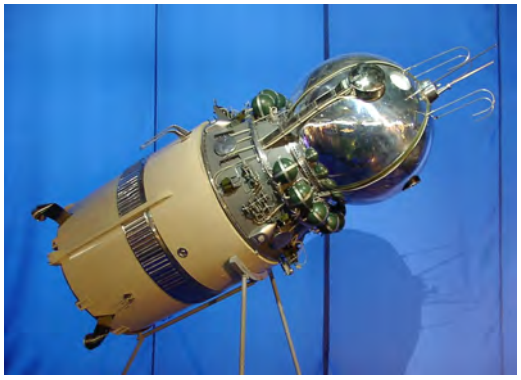

Figure 3: *Vostok 1* [10]

Figure 4: *Freedom 7* Lift-off [11]

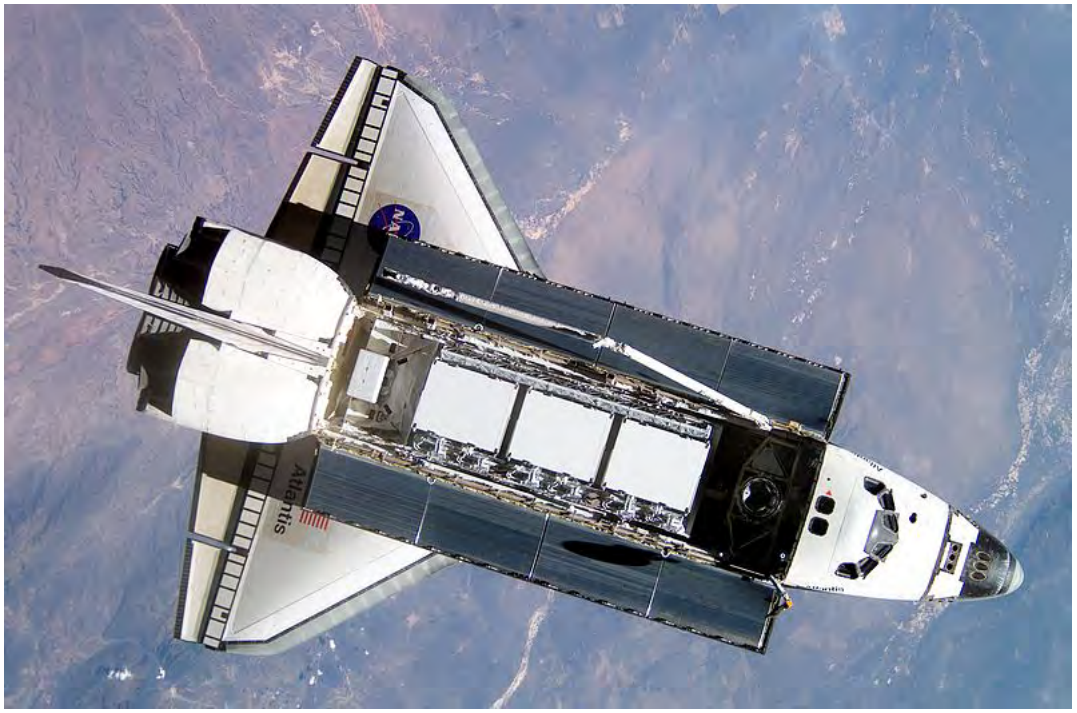

Figure 5: Space Shuttle *Atlantis* [12]

Spacecraft have been refined and have become more sophisticated thanks to the quick development of technology and further work of scientists and engineers since the 1960s. During the engineering design phase of spacecraft, a lot of different aspects are taken into account in order to build the best possible spacecraft, meaning they are able to successfully carry out their mission. For this purpose, together with the appropriate sizing and choice of materials, among others, standard atmospheric models are commonly used; they allow to analyze the interaction between the atmosphere and the space vehicles placed in it.

Atmospheric models can be analytical, semi-empirical or empirical. Analytical models are built on the mathematical dynamical equations governing the atmosphere (such as the diffusion equations). Semi-empirical models introduce measured atmospheric data into the mathematical model for its proper parametrization, accounting for altitude, longitude, solar and magnetic fluxes, among other variables. Lastly, empirical models use measured atmospheric data to formulate the functions that derive the atmospheric parameters of interest. They all aim to successfully represent either mean atmospheric conditions or specific conditions based on a particular time and location: density, temperature, pressure, and atmospheric composition. They are used in many engineering applications such as spacecraft and systems design, performance analysis and in-space operations: they help in the analysis, prediction of spacecraft flight [13] and expected lifetime. Further information on atmospheric models is discussed in sections 3 and 4, *Atmospheric Models* and *Selected Models' Evaluation Set-up*, respectively.

Furthermore, semi-empirical and empirical atmospheric modeling could be seen as an iterative process, where the first atmosphere models were fitted to rudimentary data obtained by early satellites, to be later refined thanks to more accurate data retrieved by enhanced satellites. Atmospheric model data is essential not only during the design process of spacecraft, but also for their correct operation during in-orbit missions (such as manoeuvring). It allows to estimate and account for phenomena such as atmospheric drag, which causes spacecraft orbital decay and their premature reentry during high solar activity. Actually, satellite drag data is the main source used to model the atmosphere and also the one carrying the largest error, due to it being quite hard to model; this is discussed in more detail in section 3.1.1, *Satellite Drag Data*.

Atmospheric modeling is not an easy task, mostly due to the difficulty in introducing space weather effects, whose variability is complex to monitor and predict. These models are mainly a function of date, time, altitude, latitude, longitude, and solar and geomagnetic fluxes. They are implemented in computer programs, which require the before-mentioned inputs and atmospheric conditions are given as outputs. These programs can be written in different languages, as it is discussed in section *4.1 Models' code search & Tools Used*. Performance and requirements may vary a lot between different models, so not all of them are suitable to be applied in space applications, due to their specific constraints. Since the need of high-performance and fast programs built from reliable models has arisen, comparative analyses

between current models would be extremely helpful to determine which and if any models are now obsolete, and if a better model alternative could be found. The better an atmospheric model represents reality, the better the spacecraft will operate in space. It can be anticipated that this can have a positive economic impact, as the previous knowledge of thermosphere density is essential in the estimation of satellite drag data, which causes orbital decay. This allows for a better estimation of manoeuvres, leading to fuel-saving and its consequent extension of satellite useful-lifetime. Also, it can help for a more appropriate spacecraft design. If the atmospheric conditions to be faced are known, material choice and needed size for fuel tanks, for instance, can be chosen accordingly. If the model provides poor representation of the actual atmosphere, spacecraft are deemed to not operate as desired, have a shorter life and/or to directly fail.

1.2 Objectives

The ultimate goal of this paper is to find, if possible, an efficient atmospheric model able to accurately represent the upper atmosphere at any location, at any time. It aims to determine whether current atmospheric models implemented in space-related applications could eventually be replaced by better alternatives or not, as well as to study their reliability, performance, limitations and potential improvements.

Firstly, an atmospheric model state of the art investigation is carried out. Its purpose is to give perspective on how these models have developed over the years, and how different agencies have involved themselves in such a task. A representative description of the Earth's atmosphere is given, as well as what an atmospheric model provides, how it is constructed and what variables affect it. The main goal of going into detail in these topics is a better understanding of how the atmosphere works and how it can be modelled.

Secondly, the current published atmospheric models are studied. Several common key factors are identified and used as classification criteria to group them. Then, a more detailed study of the most interesting and complete models is carried out.

Finally, evaluation and testing of selected models is done, if access to the code is possible. This will allow to get a closer sense of their capability, to compare the sources of data they feed on and interpret their results.

1.3 State of the Art

Since the mid 19^{th} century, standards and reference atmospheric models have been in development for different applications, such as engineering design and scientific research. In the 1920s, the first "Standard Atmospheres" were established by international agreement. After that, some countries have developed and published their own Standard Atmospheres, specially the United States [14].

The growing amount of different atmospheric models and the lack of proper documentation have prevented the general knowledge of their availability and information of their capabilities, as well as their limitations. The *Guide to Reference and Standard Atmosphere Models*, sponsored by the *American Institute of Aeronautics and Astronautics (AIAA)*, which has been the main source of information on the studied atmosphere models in this project, is a compilation of the available models which describe the physical properties and chemical composition of the atmosphere as a function of the altitude. The guide provides the main features of the models: model content, uncertainties and limitations, its basis, publication references, dates of development, authors and sponsors, model codes and sources. On the down side, with just a few exceptions, there is not available information on standard deviations from the mean values described by the models. This represents a serious deficiency that should be addressed, since it hinders quantitative assessments of uncertainties. It must be pointed out that the information provided by such guide was current at the time of its writing, but this might had changed by the time of its publication. Therefore, further research on selected models is advised before its usage.

Different organizations have been publishing their work over the years, usually providing new versions of their initial atmospheric models. The most noticeable organizations in the scope of this project are the following:

- ***COSPAR***: the *Committee on Space Research* was established by the *International Council of Scientific Unions (ICSU)* in an international meeting in London in 1958, after *Sputnik* was successfully launched. COSPAR's main purpose is to promote scientific space research on an international level, emphasizing on result exchange and problem discussion on space research [15].

  (1) *COSPAR International Reference Atmosphere*, *CIRA*, has provided several editions of its empirical models of atmospheric temperature and density from 0 km to 2,000 km: *CIRA 1961, CIRA 1965, CIRA 1972, CIRA 1986* and the most recent, *CIRA-08 (CIRA 2008)*. *CIRA* models combine different atmospheric models thanks to the contribution of many scientists. The model provides atmospheric temperature, density and composition but it does not give neutral winds. As it was mentioned before, one of its main limitations is that it does not provide standard deviations from the mean values of its output parameters. Also, the quality of the database that feeds the model inputs is variable. It is divided in three parts, depending on the altitude and what is being model [14]:

  Part I, *Models of the Thermosphere*. Chapter 1 describes the empirical thermospheric model like Hedin did on his *Mass Spectrometer-Incoherent Scatter, MSIS-86 Thermospheric Model*, to be used exclusively for altitudes above 120 km. Chapter 2 complements it with the theoretical models by Rees and Fuller-Rowell. The thermospheric model is published as several representative tables and figures retrieved by a FORTRAN program. Part

I is of most interest for the present project, as it will be discussed later on.

Part II, *Models of the Middle Atmosphere*. It describes the atmosphere below 90 km and for applications between 90 km and 120 km, which are called "merging models".

Part III, *Models of trace constituents*: It provides model information on the composition of the atmosphere; ozone, water vapor, methane, etc.

(2) The *COSPAR* in collaboration with the *International Union of Radio Science (URSI)* has published several versions of the *International Reference Ionosphere (IRI)*, which is an empirical model of the ionosphere. In the 50 - 2,000 km altitude range, *IRI* describes electron density and temperature, ion density and temperature and electron content for any given location, time and date [14].

- ***NASA/MSFC***: the *National Aeronautics and Space Administration (NASA)* was created in 1958. It serves as the U.S government agency to care for air and space science and technology, as well as space exploration and research [16]. NASA's *Marshall Space Flight Center (MSFC)* is in charge of building engines, vehicles and space systems among others. It does research on spacecraft propulsion, and the *Space Launch System* is being developed at the center [17].

  (1) the ***Global Reference Atmospheric Model, GRAM*** is NASA's *Marshall Space Flight Center* atmospheric model. It is used by government agencies, industries and universities for space-related applications, including vehicle design and performance criteria.

  It allows for the determination of monthly mean pressure, density, temperature, wind velocity and wind shear components, as well as their standard deviation values thanks to this model's simulation of "random perturbation" profiles about mean conditions. It works for any month, at any altitude and location in Earth's atmosphere, along any trajectory: it does not have to be linear. It also gives the atmosphere composition, including water vapor [14].

  GRAM-99 is based on the *MET* model in the 120-2500 km range. It models temperature and density variation which depend on solar and geomagnetic activity, diurnal, seasonal and latitudinal variations. *GRAM-07* is an enhanced version of *GRAM-99*, containing several new features and updated versions of its basis models [14].

  (2) the ***Marshall Engineering Thermosphere Model, MET***. It has several versions, and it consists of a computer program that models, in the 90-2500 km region, the exospheric and local temperature of the atmosphere, the number density of the atmospheric constituents, average molecular weight, total mass density and total pressure, among others. These calculations are

done as a function of latitude, longitude, time and solar flux and geomagnetic indices [14]. *MET* is an empirical model based on the ones developed by L. G Jacchia, which are mentioned later on. It is important to mention *MET-V2.0*, and *MET-2007*, which is an improved version of the former.

(3) the ***NRLMSISE-00 Thermospheric Model, 2000***. It is a product of *NASA* together with the *Naval Research Laboratory*. The *Mass Spectrometer and Incoherent Scatter Radar Extended* is an empirical model that provides neutral temperature and the density of atmospheric constituents in the 0-1400 km altitude range. As an input to the model, day, time, altitude, longitude, local solar time, magnetic index and 10.7 cm solar radiation flux index are to be provided. It is an extension of Hedin's *MSIS-86* and *MSISE-90* which uses data measured by satellite, among others.

- ***Air Force Research Laboratory***: *AFRL* is a research organization created in 1997, whose purpose is to lead the discovery, development and integration of war-fighting technologies to the U.S air, space and cyberspace forces [18]. Together with the *Space Vehicles Directorate*, they have created the stand-alone interactive program ***SHARC Atmosphere Generator, SAG***. *SAG* is a combination of several atmospheric models, like *MSISE-90*. It generates a profile for infrared radiation (IR) and the structure of the upper atmosphere. Having as an input the day, time, solar and geomagnetic activities, among others, it models temperature and the variability of the major atmospheric components density. On the down side, it does not predict, it only provides estimates of the outputs in the inputs. As any other model, it has the same uncertainties as the databases it feeds on.

- ***Smithsonian Astrophysical Observatory***: *SAO* was founded in 1890 as the research unit of the *Smithsonian Institution*, and its main focus is the study of solar radiance, and astronomy and astrophysics research [19].

  SAO has sponsored several versions of ***Jacchia Static Models of the Thermosphere and Exosphere With Empirical Temperature Profiles***, written by L.G Jacchia. The *Jacchia* models give tables of temperature, composition, density of atmospheric constituents as a function of height, in the 90 - 2500 km altitude range. Also, it provides auxiliary tables that are used to evaluate diurnal, geomagnetic, semiannual and seasonal-latitudinal effects. It is based on satellite drag data derived from ground-based tracking of several specific SAO's satellites. *J70, J71 and J77* are to be mentioned, as they are improved versions of the former.

- **Department of Defense & U.S Air Force Space Command**: The *U.S Department of Defense* was established in 1949 and has the three military branches under the control of its Secretary of Defense: Army, Navy and Air Force. Its mission is to provide the appropriate military forces to protect America. The *Air Force Space Command* was established in 1982 and it is in charge of giving space forces support and space control [20]. The collaboration

of both agencies has sponsored further revised versions of the *Jacchia* models:

(1) the ***Jacchia-Bowman Empirical Thermospheric Density Model*** follows *CIRA-72* for the formulation of the diffusion equations. It includes corrections on temperature for diurnal and latitudinal effects and on high altitude density, among others. *JB2008* is an improved version of *JB2006* [14].

(2) the ***U.S Force High Quality Accuracy Satellite Drag Model (HASDM)*** is used to obtain the global distributions of total neutral density and temperature from satellite drag data.

2 Atmosphere Description

The term *atmosphere* is highly used in the following paper, therefore, it seems necessary to provide a detailed description of it.

A celestial body's atmosphere refers to the complete set of gas layers surrounding the body, which is held in place by the its gravity. When applying this definition to Earth's atmosphere, one finds that its layer of gases is commonly known as *air*.

Earth's atmosphere is crucial to make this planet habitable, briefly [21]:

- **Role on the Water Cycle**: the atmosphere represents an important water reservoir; it spends a great amount of time in the atmosphere, mostly as water vapour but also in the shape of clouds.
- **Ozone layer**: O_3 is the ozone molecule found in the stratosphere, which is in charge of absorbing the high-energy ultraviolet (UV) radiation coming from the Sun. This radiation contains the most harmful rays to Earth's living species.
- **Greenhouse effect**: Greenhouse gases (water vapor, carbon dioxide, methane and ozone) keep the Earth's surface within an acceptable temperature range through heat retention, and reduce the diurnal temperature variation.

2.1 Earth's Atmosphere Composition and Structure

The two main components of the Earth's atmosphere are nitrogen (78%) and oxygen (21%). The remaining (1%) is made up by several inactive gases, such as argon, neon, helium, hydrogen and xenon and some others whose concentration varies, such as water vapor, carbon dioxide, methane, ozone, nitrous oxide and chlorofluorocarbons. Even though water vapor and carbon dioxide appear in very small amounts, they are of great importance due to their ability to absorb heat (greenhouse gases) [22].

Earth's atmosphere goes from the Earth's surface extending up to at least 500 km. Since air pressure and density decrease with altitude, the atmosphere is differentiated in several layers based upon the more-complex profile exhibited by the temperature. The five main layers are [23]:

- **Troposphere, 0 km - 14.5 km**: it is the densest layer of the atmosphere, containing three-quarters of it and it is where the weather happens, and where commercial aircraft fly. Its upper bound is the *tropopause*, where the temperature stops decreasing and remains constant until it begins to increase, meaning the next layer has been reached.
- **Stratosphere, 14.5 km - 50 km**: the previously mentioned Ozone layer is contained at this level. The Ozone layer absorbs UV radiation, which leads to the increase in temperature. Its upper bound is called the *stratopause*.

- **Mesosphere, 50 km - 85 km**: Again, temperature drops with increasing altitude in this layer up to its upper bound, the *mesopause*. It is where meteors burn up.
- **Thermosphere, 85 km - 600 km**: the height of its upper bound, the *thermopause*, varies with changes in solar activity. As it is also the lower bound of the Exosphere, it is also known as the *exobase*.

  In this layer, temperature increases with altitude due to the extreme low density of its molecules: it can reach a temperature of 1,500 ºC. Such molecules are so dispersed that they are not able to conduct sufficient energy to/from the skin; it would not feel hot to a human.

  This layer is of special interest since it is where most LEO satellites are placed, like the *ISS*. LEO is a geocentric orbit covering from 160 km to 2,000 km above the surface. Also, it is where aurora phenomena occur.

  The **ionosphere** is a secondary layer distinguished not for its temperature profile, but for being an ionized region by solar radiation. It overlaps the mesosphere and the thermosphere, extending from 48 km to 965 km. It is a dynamic region whose size varies depending on the wavelength of the absorbed solar radiation. It is the key region for radio communication.

  The **magnetosphere** is worthwhile mentioning. It is the area of space surrounding an astronomical object/planet controlled by its magnetic field. Earth's magnetosphere is full of *plasma*, an ionized gas which consists on positive ions and free electrons in such a proportion that produces no electrical charge: it is a neutral medium. The magnetosphere's innermost layer is the ionosphere and above it resides the plasmaspehere, which contains the coldest plasma [24]. Strictly speaking, the upper atmosphere is *plasma* weakly ionized at a few hundred kilometers of altitude and highly ionized at a few thousand kilometers [25], since at higher altitudes the atmosphere receives more direct sunlight. Figure 6 shows how Earth's magnetosphere works as a shield against solar wind (streams of charged particles going from the Sun into space).

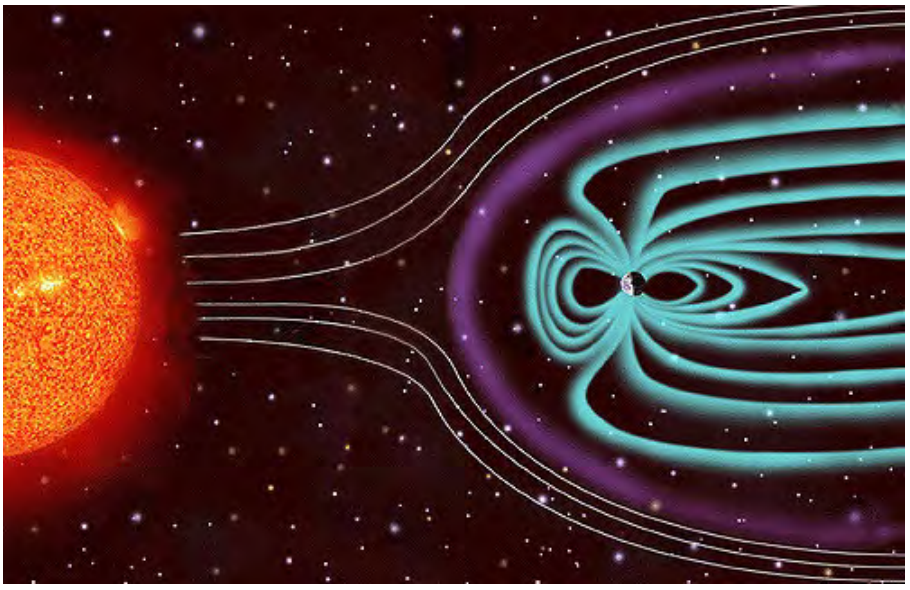

Figure 6: Solar wind impacting on Earth's magnetosphere [26]

- **Exosphere, 600 km - 10,000 km**: it is the upper limit of Earth's atmosphere. Its atoms and molecules are of very low density. They are so far apart they can travel hundreds of kilometers without colliding. Therefore, the Exosphere does not longer behave as a gas and its particles escape into space following ballistic trajectories.

  See Figure 7 for a clearer view of these layers.

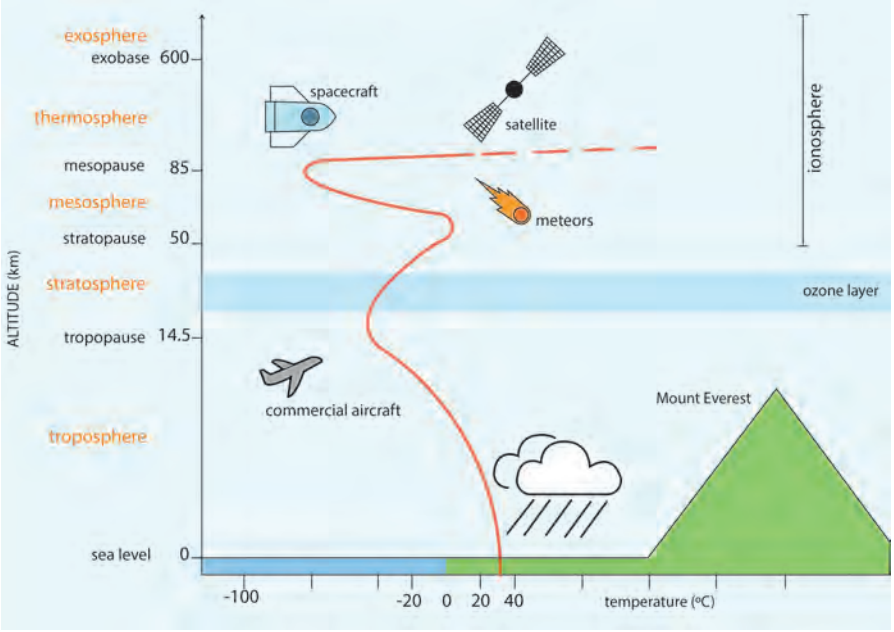

Figure 7: Earth's atmosphere layers

2.2 Outer Space

After having defined the different layers that conform the atmosphere, the question "where does *outer space* begin" arises. This boundary has not been well defined, so the answer depends on who is asked.

On the one hand, the *Kármán Line* is commonly used to define such boundary. The *Kármán Line* lies at 100 km above mean sea level, where the atmosphere becomes so thin that conventional aircraft is no longer able to maintain flight. Beyond this imaginary line, conventional aircraft would need to reach at least orbital speed to maintain flight, or they would fall [27].

On the other hand, *NASA* defines space to start at 80 km above the Earth's surface. This definition would not consider some orbiting satellites nor the *ISS* as spacecraft [27]. Therefore, for this atmospheric model study, the *Kármán Line* has been set to define the boundary for outer space.

3 Atmospheric Models

As it was mentioned before, semi-empirical and empirical models are based on observations rather than in full theory or logic, and they predominate over purely analytical models. They are based on an extended data compilation from the soon-to-be-explained measurement techniques, for which a fitting is developed for every dependent variable of the model (density, temperature, etc). Usually, one model is based on a combination of other older models, integrating advantages of each of them. They can also feed on different databases available, and their outputs can be compared to one another to check their validity.

Atmospheric modeling could be considered as an iterative process, which is based on building more accurate models based on older atmospheric fittings. In a simplified manner, this process can be summed up in the following steps:

1. Atmospheric data is measured using different techniques.

2. Data is fitted into different profiles for the desired model outputs (density, temperature, etc).

3. Model is used to shape the atmosphere, where spacecraft are sent to.

4. New data is measured, so model accuracy can be checked comparing it to the model estimation.

5. The fit for the model is enhanced by the new data, which allows for a further observation of atmospheric dependence on different factors, as day, time, altitude, latitude, solar radiation flux index and magnetic index. It is worth to mention that models inherit their databases' uncertainty, so thanks to technology improvement, empirical data uncertainty is decreased leading to high-accuracy measurements.

6. Back to step number 3.

3.1 Data Acquisition

The formulation of the empirical functions used to derive the atmospheric parameters of the different models can be based on data obtained from satellite drag, mass spectrometry and/or incoherent scatter, and accelerometer data. Then, its accuracy can be checked by comparing the model's results to data directly extracted from these techniques. The explanation of such techniques is therefore considered necessary for a better understanding of atmospheric modeling.

3.1.1 Satellite Drag Data

Satellite drag data is one of the main sources to model the atmosphere. In other words, atmospheric density is inferred from analyzing the satellite orbital decay caused by aerodynamic drag.

The term *drag* refers to the force acting on an object moving through a fluid in the opposite direction. Aerodynamic drag depends on the properties of the fluid and on the shape, size and speed of the object, following (1),

$$D = \frac{1}{2}\rho v^2 C_D A \tag{1}$$

where ρ is the density of the fluid, v is the speed of the object relative to the fluid, A is the cross sectional area of the object and C_D is the drag coefficient, a dimensionless number. It is important to point out that the drag coefficient is a function of the satellite's configuration and of the gas the satellite is interacting with. Therefore, it is necessary to have some knowledge on the atmosphere in order to determine the drag coefficient. Such coefficient is determined experimentally if possible, but since the conditions of a satellite in orbit are so different from those reproduced in a laboratory, satellite drag coefficients are to be evaluated just by theory [25].

It is appropriate to introduce now the concept of *solar activity* during the *solar cycle*. The *solar cycle*, which lasts about 11 years, is the variation of the Sun's magnetic field as its poles switch places: the north pole becomes the south pole and vice versa. This change in the solar magnetic field is responsible for *solar activity*, which includes solar flares, coronal mass ejections, high-speed solar winds and solar energetic particles. The *solar cycle* can be monitored by the amount of *sunspots* existing on the Sun's surface. These *sunspots* appear due to very strong magnetic field lines emerging from within the Sun and piercing through its surface in arbitrary areas, inhibiting convection in such areas and resulting in considerable lower temperatures in comparison to their surroundings. Therefore, *sunspots* manifest as visible temporary dark regions, appearing always in pairs (N-S) [28], see Figure 8. The beginning of the cycle corresponds to the *solar minimum*, when the Sun has the least *sunspots* and solar activity is low. With time, solar activity (due to increasing number of *sunspots*) increases until the middle of the cycle, when the *solar maximum* is reached. Then, solar activity fades until a new cycle begins with a new *solar minimum* [29].

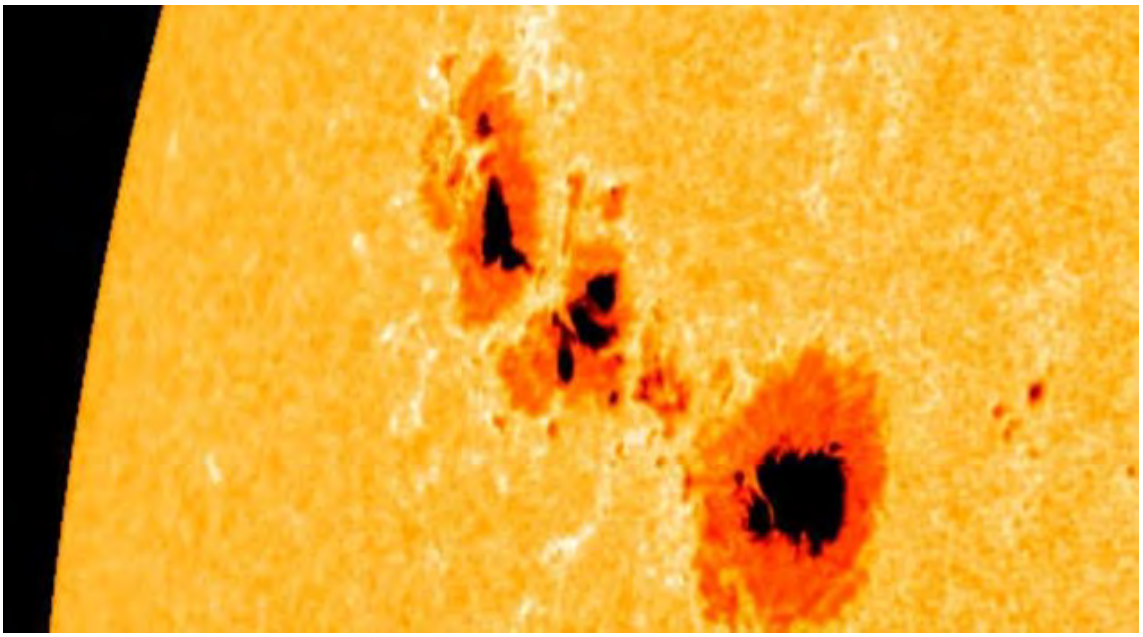

Figure 8: Sunspots on the Sun's surface [30]

EUV radiation (solar photons) and the solar wind (corpuscular radiation) are the two main solar activities that affect thermospheric density:

- EUV radiation predominates since it accounts for 80% of the energy input received by the thermosphere from the Sun, determining its basic structure. EUV radiation changes over a 27-day solar rotation period and day-to-day dependencies, which makes the thermosphere to be a dynamic region at low altitudes. Due to the complexity of obtaining observational data of this phenomenon, the $F_{10.7}$ radio flux is commonly used as an indicator for solar EUV heating, measured in solar flux units (sfu), where 1 sfu = 10^{-22} W m^{-2} Hz^{-1}. It can also be represented as a running 81 day average, denoted by $\bar{F}_{10.7}$ [31].

  The evolution with time of the before-mentioned *sunspots* and the $F_{10.7}$ solar index can be seen in Figures 9 and 10. Since in 2008 the current *solar cycle 24* began, it is observable that the number of *sunspots* were lower as well as the solar flux, then incremented in the following years, and are now decreasing again as the solar cycle is coming to and end.

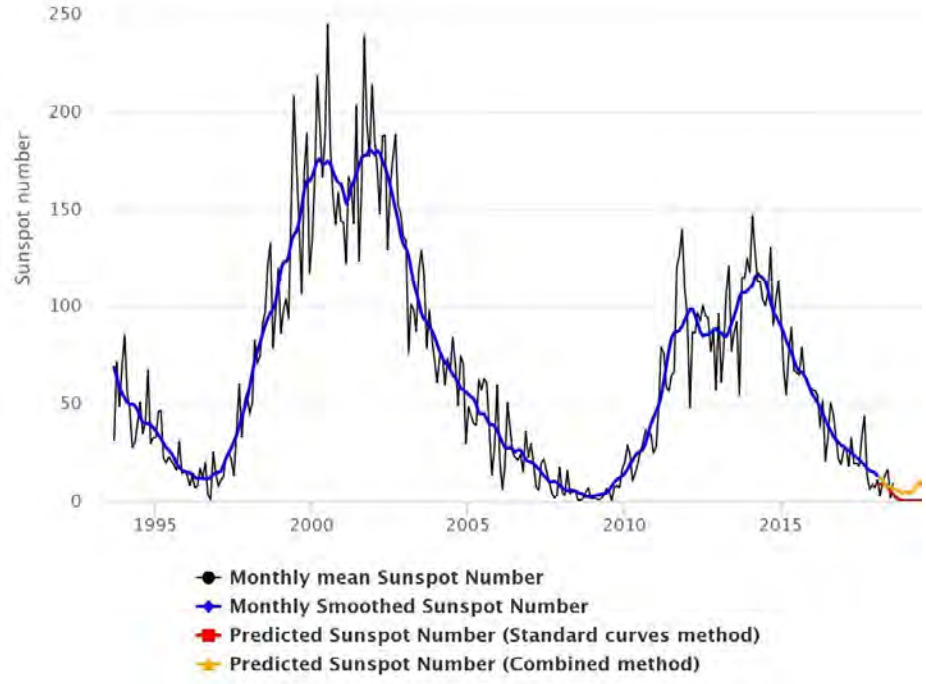

Figure 9: Solar Cycle Progression - Sunspot Number [32]

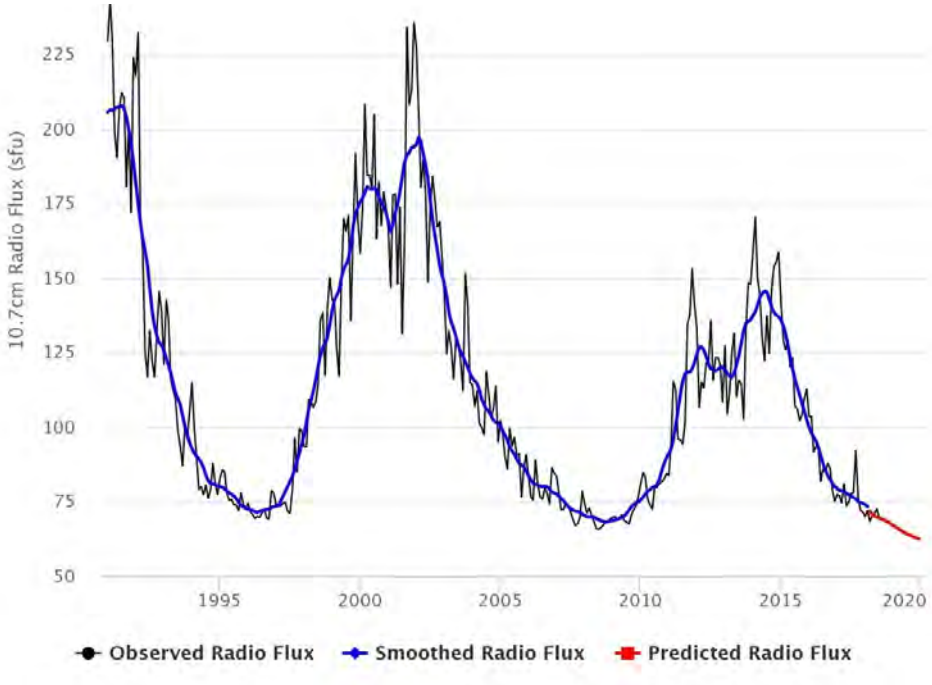

Figure 10: Solar Cycle Progression - $F_{10.7}$ Radio Flux [32]

- Auroral processes (i.e auroral heating) are related to solar wind, and make the thermosphere a dynamic region at high altitudes [31]. Geomagnetic activity is measured by the quasi-logarithmic geomagnetic planetary index, *kp*. It represents a worldwide average of geomagnetic activity measured below the auroral zones every 3 hours. Furthermore, every 3-hour Kp value is converted to a linear equivalent, which is known as the geomagnetic planetary amplitude, *ap*. The average of the 8 daily *ap* values leads to a daily planetary amplitude *Ap* [33]. The conversion Table 1 from Kp to *ap* values is given by *SpaceWeatherLive* [34], agreeing with NOAA [35].*Ap* index is usually used as a proxy for geomagnetic activity needed as input in atmospheric models, as further mentioned in section *4.2 Required Model Inputs*.

Kp	0o	0+	-1	1o	1+	-2	2o	2+	-3	3o	3+	4-	4o	4+
Kp in decimals	0.00	0.33	0.67	1.00	1.33	1.67	2.00	2.33	2.67	3.00	3.33	3.67	4.00	4.33
ap	0	2	3	4	5	6	7	9	12	15	18	22	27	32
Kp	-5	5o	5+	-6	6o	6+	-7	7o	7+	-8	8o	8+	-9	9o
Kp in decimals	4.67	5.00	5.33	5.67	6.00	6.33	6.67	7.00	7.33	7.67	8.00	8.33	8.67	9.00
ap	39	48	56	67	80	94	111	132	154	179	207	236	300	400

Table 1: Conversion from Kp to *ap* values

As defined in *NRLMSISE-00 Empirical Model of the Atmosphere: Statistical Comparisons and Scientific Issued* [36], Table 2 represents the classification of solar and geomagnetic activity based on $F_{10.7}$ and *Ap* indices.

$F_{10.7}$ **Solar Activity**			*Ap* **Geomagnetic Activity**	
Low	$F_{10.7}$<75		Quiet	*Ap*<10
Moderate	75<$F_{10.7}$<150		Moderate	10<*Ap*<50
Elevated	150<$F_{10.7}$<190		Active	50<*Ap*
High	190<$F_{10.7}$			

Table 2: Solar and Geomagnetic Activity Bins

Even though air density in the thermosphere is very low compared to that near Earth's surface, it still produces considerable drag on satellites travelling in LEO, slowing them down and pulling them closer to the Earth. As a consequence of the Sun emitting more energy to the upper atmosphere, the temperature increases and the density decreases. Furthermore, atmosphere layers are no longer as strongly attracted to the Earth by its gravitational field (they weigh less) as they were before, allowing for the low-density air layers in LEO rise and to be replaced by higher-density layers that were beneath the former. In other words, the

thermosphere puffs up when heated by EUV and x-radiation, as it can be observed in the simplified sketch of Figure 11.

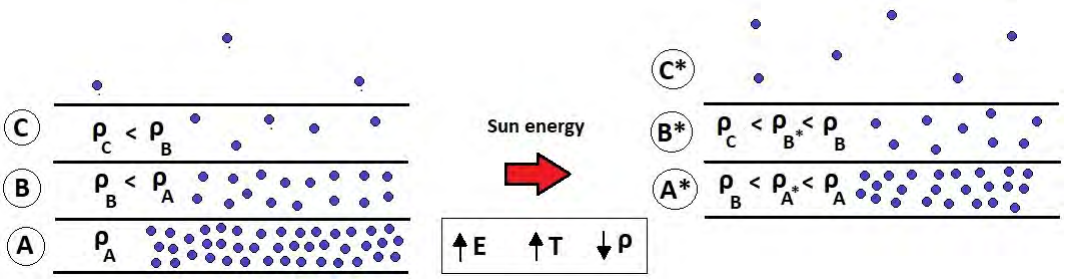

Figure 11: Sketch of thermosphere puff-up

Consequently, the drag force on satellites increases in agreement with equation (1). As a result, satellites need to be re-boosted to their orbits to make up for atmospheric drag. Together with the long-term effects of the solar cycle, the interaction between the solar wind and Earth's magnetic field during geomagnetic storms leads to short-term increases in temperature and density, followed by a stronger aerodynamic drag and satellite orbital decay [37]. It is important to point out that the study (more specifically, the prediction) of the solar cycle is essential to determine the lifetime of satellites in LEO. For example, in the long run, strong solar activity can cause early reentry of spacecraft due to the increase of atmospheric drag and consequently, orbital decay.

Not being able to properly model atmospheric drag is one of the main sources of error in atmospheric models, due to the before mentioned complexity of the Sun-driven variations of the neutral atmosphere.

3.1.2 Mass Spectrometry

"A mass spectrometrist is someone who figures out what something is by smashing it with a hammer and looking at the pieces" [38]. *Mass Spectrometry* is an analytical technique that allows to determine a molecule's structure and elemental composition. A mass spectrometer ionizes the chemical substance sample and uses an electric and/or magnetic field, in vacuum, to measure their mass-to-charge ratio. It classifies the gaseous ions based on their mass-to-charge ratio and relative abundance. The mass spectrum of the molecule presents this information in an ion abundance versus mass-to-charge ratio plot [39].

A mass spectrometer has three main components [39], as Figure 12 represents:

- Ion Source: it ionizes the chemical sample.
- Mass Analyzer: the product ions are sorted and classified according to their mass-to-charge ratio.

- Detector: the relative abundance of the resulted ion species is measured.

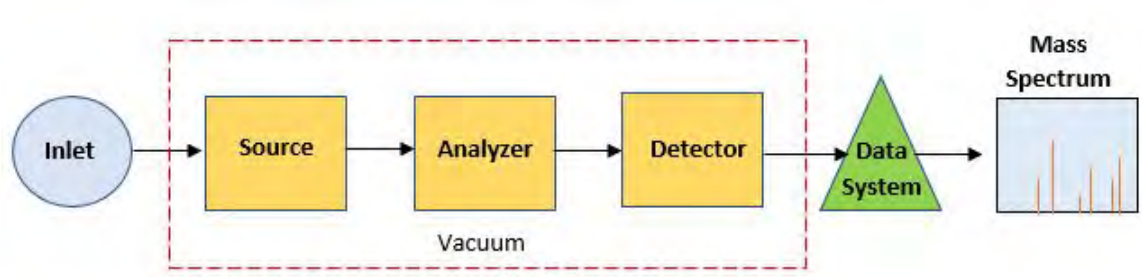

Figure 12: Mass Spectrometer sketch

Mass spectrometers are highly used in space applications, as satellites can be equipped with them in order to identify the particles they intercept in the atmosphere. Therefore, mass spectrometry is a satellite-based technique for examining space, providing information at different altitudes, latitudes, longitudes, solar activities and seasons.

3.1.3 Incoherent Scatter Radar

Incoherent scattering is based on the fact that free charged particles are accelerated in an electromagnetic wave field and excited to radiation, where the incident and emitted waves' frequency is the same but have different spatial directions [40]. In other words, a radar transmits a signal wave at a target matter. The electrons of such matter accelerate due to the incident wave and emit a much weaker response signal: the wave is reflected and scattered [41].

The *incoherent scatter radar (ISR)* is a ground-based technique used in space applications to study the ionosphere, where the incoherent scatter comes from its electrons or plasma. It measures electron and ion temperature, velocity and number density. This technique is able to study how the ionosphere and upper atmosphere are affected by solar radiation coming from the Sun and particles making it through Earth's magnetosphere, and energy, usually coming from denser lower atmosphere layers coming in the form of waves [41].

As its own name suggests, ISR consists on a radar having one or more antennas and a very powerful transmitter. They are usually monostatic: they have one antenna working as the transmitter and as the receptor [41]. Figure 13 shows the Millstone Hill radar, from the MIT Haystack Observatory in Massachusetts, U.S.

Figure 13: Haystack Observatory: Millstone Hill Radar [42]

3.1.4 Satellite-borne Accelerometer

An accelerometer is an electromechanical device capable of measuring linear and angular acceleration based on the inertial reaction of a proof mass [43]. In other words, it measures the vibration/acceleration of a moving structure.

Atmospheric density can be derived from satellite-borne accelerometer data. An example of such device in space applications is the *STAR* accelerometer on-board the *CHAMP* satellite, whose mission was to do research on the atmosphere and ionosphere (2000-2010) [44]. Also, the *Super-STAR* accelerometer on twin *GRACE* satellites is to be mentioned, as data from both missions is used for the development of atmospheric models.

The *CHAMP* satellite was equipped with several devices to observe the Earth: magnetometers to map its magnetic field, digital ion-drift meter to measure its electrical field, among others. The high-accuracy *STAR* accelerometer was integrated at its center of mass to avoid disturbances from centrifugal and angular accelerations. *STAR* measured non-gravitational accelerations on *CHAMP* due to air drag, solar radiation pressure and attitude and orbit control system (AOCS) impulses in LEO [45]. Together with the on-board GPS and SLR tracking systems,

orbit positioning was precisely determined [46] and atmospheric density is derived.

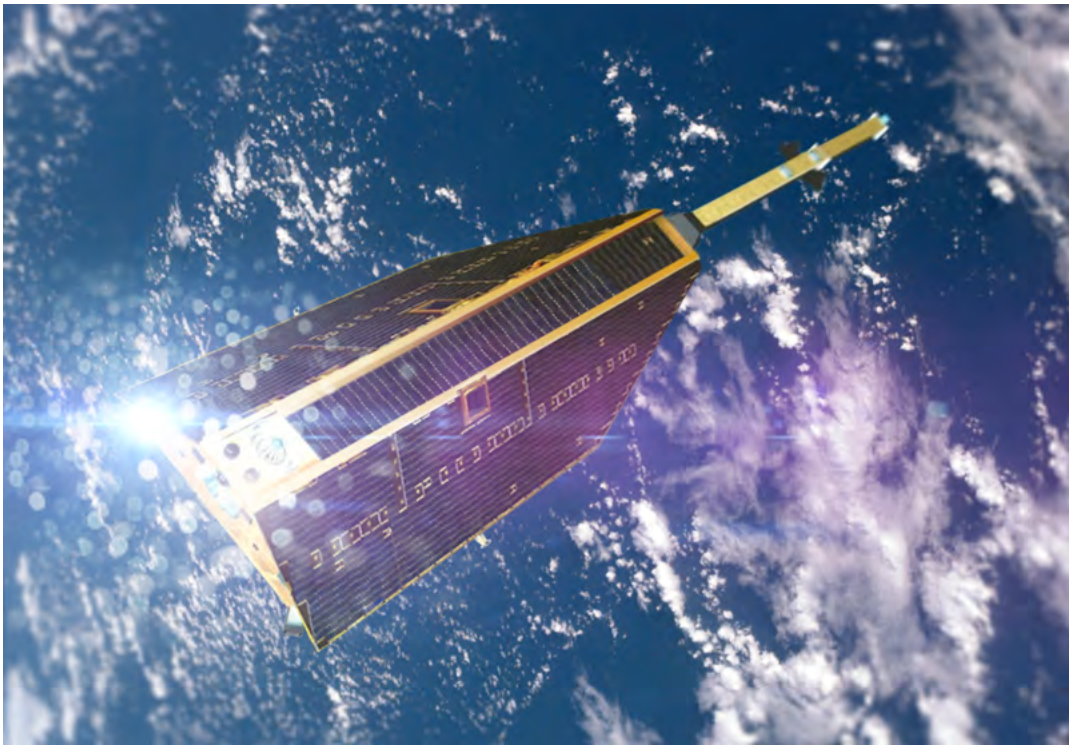

Figure 14: *CHAMP* satellite [47]

3.2 Classification

The *Guide to Reference and Standard Atmospheric Models* [14] classifies the collected models in Global, Regional, Middle Atmosphere, Thermosphere, Range and Planetary models, which has been quite helpful for their evaluation.

While reading such guide, three main key factors emerged and helped to dismiss the models of no interest in the scope of this project: being able to represent the upper atmosphere as precisely as possible with just one model.

3.2.1 Key Factors

- Altitude range: since the main goal is the appropriate modeling of the atmosphere for space applications, the altitude range covered by the models must cover altitudes at least above the Kármán Line (above 100 km), where satellites and spacecraft travel in LEO.
- Global aspect: the models must not be developed for a specific region of Earth. They must work for any latitude and longitude on Earth, giving it a global aspect. This avoids having to choose/change between different models

depending on where the spacecraft is situated at the time, which could result in management and performance problems. The most interesting and valuable advantage of global models is their performance, even if region-specific models could offer slight higher precision in some cases.

- Permanent aspect: the models must work for any season of the year, since it has been mentioned that they highly depend on the solar cycle. Therefore, the difficulties and errors of the models that may unable them to be permanent in time must be overcome.

3.2.2 First Discard Process

Based on the three main key factors, a first discard process was carried out. Following the *Guide to Reference and Standard Atmospheric Models* [14]:

- Global models

  The *ISO Reference Atmospheres for Aerospace Use, 1982* and *ISO Standard Atmosphere, 1975* only cover from the Earth's surface up to 80 km, not even reaching the Kármán Line.

  The *NASA/GSFC Monthly Mean Global Climatology of Temperature, Wind, Geopotential Height, and Pressure for 0-120 km, 1988* as its own name indicates, it only covers the 0-120 km altitude range. It does cover 20 km of outer space above the Kármán Line, but it was not believed to be enough considering the thermosphere goes up to 600 km and LEO starts at 160 km.

  The *U.S Standard Atmosphere 1962* and *1966* do comply with the altitude range going up to 700 km. On the other hand, they are described to be very unreliable above 90 km due to the varying degrees of confidence in their data. The *U.S Standard Atmosphere, 1976* also complies with altitude range conditions but it is described to be insufficiently representative of global conditions, due to the spotty geographic coverage of its rocket network.

  The *International Reference Ionosphere 2007* is discarded since it is an empirical standard model of just the ionosphere. It does have good capabilities to model electron density and temperature, among others, but it does not model atmospheric neutral density, temperature and constituents.

  The *Exospheric Hydrogen Model, 1994* is also discarded since it only models the exospheric hydrogen density.

- Regional models

  All regional models are discarded as they have been developed to model just a specific region and or conditions, i.e *China National Standard Atmosphere,*

1980 and *Proposed International Tropical Reference Atmosphere,1987.*

- Middle Atmosphere Models

  All middle atmosphere models are dismissed since they extend up to 120 km, at most. As it was mentioned before, covering just 20 km in space is not considered useful in the scope of the project. For example, *Extensions to the CIRA Reference Models for Middle Atmosphere Ozone, 1993* and *ISO Middle Atmosphere-Global Model at Altitudes Between 30 km and 120 km, and Wind Model at Altitudes Above 30 km, 1996.*

- Thermosphere Models

  The *AFGL Model of Atmospheric Structure, 70 to 130 km, 1987* is discarded for the same reason as the middle atmosphere models.

  The *Russian Direct Density Correction Method (DDCM)* determines near real-time corrections to an density model. Therefore, it is not considered as an atmospheric model itself but as an aid for error estimation to other models.

  On the same line, the *Horizontal Wind Model (HWM), 1993* just represents Earth's horizontal wind fields in the 0-500 km altitude range.

- Range Models

  All range models are discarded as they have been developed for specific geographic location, i.e *Twenty-two Range Reference Atmospheres, 2006* and *Reference Atmosphere for Edwards Air Force Base, California, Annual, 1975.*

- Planetary Models

  Since Earth is the planet in the scope of the project, any other atmospheric model developed for a different planet is of no interest, like *NASA/MSFC Mars Reference Atmospheric Model (MARS-GRAM), 2001.*

3.3 Second Discard Process

Once the number of models is narrowed down, it is necessary to carry out a deeper investigation on their dependencies, properties, accuracy and performance in order to select the most interesting ones. Even though every selected model up to this point covers the altitude range condition and is global and permanent, several different factors might make some models more attractive than others. As a general point in

common, all these models need to be provided with several of the following inputs: the day of year, altitude, time and solar activity indices, among others, in order to generate their atmospheric profiles. The most determinant factors on this second discard process are the present acceptance of the model and how focused it is on representing atmospheric conditions.

The family models to choose from are *CIRA, GRAM, SAG, GOST, Drag Temperature Model (DTM), Jacchia* and *Jacchia-Bowman* models, *MET, NRLMSISE* and *HASDM*.

- As far as *CIRA 1986* is concerned in the scope of the project, its only useful part would be *Part I: Models of the Thermosphere*, to be used above 120 km. As it was mentioned before, this part is identical to NASA's *MSIS-86*. Therefore, it would be preferred to study more in depth the *MSIS-86* model or an improved version of itself.
- *Jacchia* models are discarded due to the *Jacchia-Bowman* ones giving improved results while using *Jacchia* models as their basis.
- *SAG* is discarded since its main focus is the modeling of radiance variations in the atmosphere. It is preferred to study models that are more centered in the scope of the project, in other words, that above all aim to represent temperature, density and atmospheric composition.
- The *HASDM* is able to reduce satellite drag data model errors in real-time, thanks to the *Dynamic Calibration Atmosphere (DCA)* satellites used for drag analysis, whose data is used for density correction. Despite its success to improve orbit determination, it has been considered it to be more of an "aid" to other models, rather than of interest to be studied as a model itself.

Finally, it was determined it would be of interest to study in more detail and implement at least three of the following models: *NRLMSISE-00, GOST-2004, MET - 07, JB-2008*, *GRAM-2010* and *DTM-2013*.

4 Selected Models' Evaluation Set-up

Before model implementation, it was necessary to obtain their codes and to find suitable satellite-measured data for the comparative analysis that would enable a meaningful test bench.

4.1 Models' code search & Tools Used

It is a fact that obtaining the codes of the models was neither an easy task nor always possible, as several different reasons can interfere in their accessibility.

Unfortunately, *NASA's GRAM* was requested on *NASA's* official site (after registration), with no results (in time). *Dr. Paul J. Cefola*, a consultant in Aerospace Systems, Spaceflight Mechanics and Astrodynamics and one of the research scientists in charge of the development of the *GOST* model from the *University at Buffalo, US* was contacted. Even though he did send some interesting papers with information about the model, he did not give access to the code. He showed an interest to create a MATLAB version of it, but this task is out of the scope of the project due to its complexity.

On the other hand, *NASA's MET-07* was requested and it was accessible in time for use [48]. It was supplied in FORTRAN and it was compiled to use as an executable program. *NRLMISISE-00* code is of public access and was found in several different programming languages. The MATLAB adaptation from the FORTRAN code was found at the *shared files* section in *MathWorks*. It was poorly commented and believed to be missing parts, therefore it was classified as of no use. This model was found at the *Community Coordinated Modeling Center* for its online computation and plotting [49]. The *JB-2008* is of public access and was found for FORTRAN and MATLAB at the model's official website [50]. Finally, the *DTM* is supposedly available for free download at the *Advanced Thermosphere Modeling for Orbit Prediction, ATMOP* official website [51]. The official registration in *ATMOP* is necessary, and for some unknown reason registration was not possible. *Dr. Sean Bruinsma*, head of the *Space Geodesy Office* at the *Centre National d'Etudes Spatiales (CNES)* in Toulouse was contacted. He gave access to *DTM* FORTRAN subroutines as well as some guidelines on its input parameters. Also, there is an option for running the model online at the *ATMOP* website [51].

Table 3 sums up code availability and language of the models, being marked in green the sources actually used for the implementation of each model. The reasons behind using the online modelling interfaces for *NRLMSIS-00* and *DTM* are either finding poor-commented codes that are very hard to follow (variables may not be explained) or due to not being familiar enough with FORTRAN and C programming tools to successfully work out the codes.

As far as *JB-2008* is concerned, it is a built-in MATLAB function. A test script was

found in *MathWorks* [52] that guides the user through every step of the computation. Furthermore, this script allows for the correct feeding of the parameters to the function, since they have to agree in units. It even has different databases in its work-space to read solar and geomagnetic indices automatically, whose text files are available for download at the same official website where the code was found. This will be later discussed.

Models	Code Availability			Code Language		
	Online	**Upon Request**	**Free download**	**Fortran**	**M (Matlab)**	**C**
NRLMISISE -00	X (CCMC)		X	X	X	X
GOST 2004		X (To author: Paul Cefola)		X		
MET-07		X (NASA)		X (executable)		
JB-2008			X	X	X	
GRAM-2010		X (NASA)		X		
DTM-2013	X (ATMOP)	X (To author: Sean Bruinsma)	X (ATMOP)	X		

Table 3: Model Code Source Availability

For the comparison of the data, MATLAB is used to represent the data in graphs. These provide visual insight of how these data differ from each other.

4.2 Required Model Inputs

As user-provided inputs, the following independent variables are usually required (maybe not all of them) for the model to generate its output results for the desired estimation:

- Date: year, month and day.
- Time (UT): Universal Time is a solar time standard, measured by the stars. It refers to the average speed of Earth's rotation. A solar day is about 24 hours [53].
- Local Solar Time: related to the location of the sun: local solar noon (zero hours) is when the sun is at its highest, on observer's meridian [54].

- Latitude: geographic coordinate determining north/south degree position relative to the Equator (0 degrees).
- Longitude: geographic coordinate determining east/west degree position relative to the Prime Meridian (0 degrees).
- Altitude: position above mean sea level.
- Solar radiation flux index: $F_{10.7}$ is the most used solar activity index. Its values indicate the Sun's radio emissions at 10.7 cm wavelength, measured from the solar disk every hour. Wavelengths around 10 cm have been concluded to be the best ones to monitor solar activity [55]. It is important to emphasize that the uncertainty in the estimation of future solar EUV heat input makes it very hard to proper model atmospheric drag, and therefore, this becomes the main source of error in the models. There are databases with these measurements, such as the *RSGA, Report of Solar and Geophysical Activity* provided by the *Space Weather Prediction Center, SPWC.* [56]. On the other hand, it is common for models to need variations of the $F_{10.7}$ index, such as its monthly average or the before mentioned 81-day average. Furthermore, instead of of using the 10.7 cm wavelength emissions, they might use the 30 cm wavelength emissions, denoted as F_{30}.
- Magnetic Index (Ap): magnetic indices measure magnetic activity in an approximate 3-hour time range. Solar radiation perturbs the magnetic field, as well as irregular current systems caused by solar wind impacting on the magnetosphere, as an example [35]. The common used Ap index is defined by reference [35] as *"the earliest occurring maximum 24-hour value obtained by computing an 8-point running average of successive 3-hour ap indices during a geomagnetic storm event and is uniquely associated with the storm event"*. It represents the daily average value of geomagnetic activity. There are databases with these measurements, like *RSGA*. It can be the case where the *Disturbance Storm Time, Dst,* index is required. This index indicates the strength of the geomagnetic storm-time ring current in the inner magnetosphere [14].

4.2.1 *NRLMSIS-00* Online Model Inputs

The online *NRLMSIS-00* model has different input options, as follows:

Necessary input parameters

- Date: in the range [1960/02/14-2017/04/17] (end date is uploaded monthly)
  1. Year
  2. Month
  3. Day
- Time: to specify if universal or local.
  1. Hour of the day: in the range [1-24]

- Coordinates: to specify if geographic or geomagnetic.
  1. Latitude: in the range [-90º - 90º]
  2. Longitude: in the range [0º - 360º]
  3. Height: in the range [0 km - 1000 km]

- Profile type and its parameters: to choose from all of the above as profile type and determine:
  1. Start
  2. Stop
  3. Step-size

Optional input parameters: if these are not provided, they are automatically taken from the associated database red(not specified).

- $F_{10.7}$ daily value from previous day
- $F_{10.7}$ 3-month average - 81-day average centered on input day
- Ap daily

4.2.2 *MET-07* Inputs

- Date:
  1. Year
  2. Month
  3. Day
- Time:
  1. Hour: in the range [0 - 24]
  2. Minute
  3. Second
- Coordinates:
  1. Latitude [-90º - 90º]
  2. Longitude [-180º - 180º]
  3. Height [km]
- Solar and geomagnetic activity indices:
  1. $F10 = F_{10.7}$ solar flux
  2. $F10B = F_{10.7}$ solar flux average, 81-day centered on the input time
  2. Kp or Ap geomagnetic index

4.2.3 *JB-2008* MATLAB Inputs

It is observable how this model has introduced more space weather inputs than the others, as there are new solar indices that measured far EUV activity, and the *ap* geomagnetic index is replaced by the *Dst* index.

It is to be pointed out that the term *right ascension* is the equivalent of the geographic *longitude* in celestial coordinates. In the same way, the *declination* is comparable to geographic *latitude*.

- MJD: Date and Time in Modified Julian Days and fraction (MJD = JD - 2400000.5).
- Right Ascension of Sun [radians]
- Declination of Sun [radians]
- Right Ascension of Position [radians]
- Geocentric Latitude of Position [radians]
- Height of Position [km]
- F10: $F_{10.7}$ in [10^{-22} W m^{-2} Hz^{-1}] (Tabular time 1.0 day earlier)
- F10B: $F_{10.7}$ solar flux average, 81-day centered on the input time (Tabular time 1.0 day earlier)
- S10: EUV index (26-34 nm) scaled to F10 (Tabular time 1.0 day earlier)
- S10B: EUV 81-day ave. centered index (Tabular time 1.0 day earlier)
- XM10: MG2 index scaled to F10 (Tabular time 2.0 days earlier)
- XM10B: MG2 81-day averaged centered index (Tabular time 2.0 days earlier)
- Y10: Solar X-Ray & Lya index scaled to F10 (Tabular time 5.0 days earlier)
- Y10B: Solar X-Ray & Lya 81-day average centered index (Tabular time 5.0 days earlier)
- dT_c: Temperature change computed from Dst geomagnetic storm index

4.2.4 *DTM-2013* Online Model Inputs

Necessary input parameters

- Date: in the range [1972/01/01 - 2012/08/31]
  1. Year
  2. Month
  3. Day

- Time:
  1. Hour
  2. Minute
  3. Second
  4. Millisecond

- Coordinates:
  1. Latitude: in the range [-90º - 90º]
  2. Longitude: in the range [-180º - 180º]
  3. Height: in the range [120 km - 1000 km]

Optional input parameters: if these are not provided, they are automatically taken from the associated database red(not specified).

- Solar proxy "f" parameter: F_{30} daily observed parameter delayed by 24 hours, re-scaled to $F_{10.7}$.
- Solar proxy "fbar" parameter: F_{30} 81-day average, re-scaled to $F_{10.7}$.
- Geomagnetic proxy parameter $akp(1)$: delayed 3-hourly Kp index in the range [0.0 - 9.0] (in decimals).
- Geomagnetic proxy parameter $akp(3)$: Kp mean of the last 24 hours in the range [0.0 - 9.0] (in decimals).

  All these values are to be prepared and interpolated, which is not an easy task: 1. The solar flux has to be interpolated to the decimal date for the 81-day mean, and interpolated to the decimal date minus 24 hours for the daily flux (i.e. 1-day delayed instantaneous flux).

  It was advised by *Dr. Bruinsma* that the best results are obtained using the F_{30} radio flux from *Nobeyama* and then re-scaled to $F_{10.7}$, although both F_{30} and $F_{10.7}$ are valid for running calculations. These indices hold the following relationship:

$$F_{10.7} = -1.5998 + 1.553755 F_{30} \tag{2}$$

  2. The Kp has to be computed from similarly interpolated ap values: interpolating linearly from one to the next 3-hourly ap value, then converting to Kp.

4.3 Model Outputs

Atmospheric models aim to provide information about atmospheric conditions, such as temperature, density, and composition. Nevertheless, some models may be able

to provide more information than others. It is important to point out that since the comparative analysis is limited by the found satellite-measured data, not all the outputs are likely to be analyzed in the implementation of the models.

Table 4 resumes the models' outputs and indicates the units they use. It is observable how *NRLMSIS-00* and *MET-07* provide atmospheric composition using *number density*, whereas *DTM-2013* provides *concentration*.

Output	**Model**			
	NRLMSIS-00	***MET-07***	***JB-2008***	***DTM-2013***
Total Mass Density	[g/cm^{-3}]	[kg/m^{-3}]	[kg/m^{-3}]	[g/cm^{-3}]
Neutral Temperature	[K]	[K]	[K]	[K]
Exospheric Temperature	[K]	[K]	[K]	[K]
Nitrogen (N_2)	[cm^{-3}]	[m^{-3}]		[g/cm^{-3}]
Oxygen (O_2)	[cm^{-3}]	[m^{-3}]		[g/cm^{-3}]
Helium (He)	[cm^{-3}]	[m^{-3}]		[g/cm^{-3}]
Argon (Ar)	[cm^{-3}]	[m^{-3}]		
Atomic Oxygen (O)	[cm^{-3}]	[m^{-3}]		[g/cm^{-3}]
Atomic Hydrogen (H)	[cm^{-3}]	[m^{-3}]		[g/cm^{-3}]
Atomic Nitrogen (N)	[cm^{-3}]			[g/cm^{-3}]
Anomalous Oxygen	[cm^{-3}]			
Mean Molecular Mass				[g/cm^{-3}]
Average Molecular Weight		[-]		
Total Pressure		[Pa]		

Table 4: Model Outputs and Corresponding Units

The *ATMOP* offers three different functionalities for *DTM-2013* modelling:

1.Single call: every input is required and numerical values of the outputs are given. For air density, the percentage of error is also given.

2.Atmospheric profile: every input is required but for the altitude. It graphically gives density and component concentration distributions from 0 km to 1000 km at the date and location requested.

3.Global density distribution at a height: every input is required but for the coordinates. It graphically gives atmospheric density distribution at the required date and altitude as a function of longitude and latitude.

4.4 Test Bench Set-Up

The aim of the following test bench is to analyze how well these models are able to represent atmospheric conditions by comparing them to actual measurements.

4.4.1 Solar and Geomagnetic Activity Indices Databases

As two of the main required model inputs, solar and magnetic indices are essential. They are given in the *RSGA* provided by *Space Weather Prediction Center* within the *NOAA* [57]. It holds information from as early as 1966 up to this day.

As for the files that *JB-2008* feeds on, they are available at the model's official website [50], and they are included in the test script available for download in *MathWorks* [52]. The Earth Orientation Parameter (EOP) Data, starting in 1962/01, is provided by *CelesTark* withing the *Center for Space Standards & Innovation (CSSI)* [58]. Space weather data is given by the *Space Environment Technologies (TEC)* and is found at the model's official website [50].

4.4.2 Satellite-measurements' Databases

Searching for real thermospheric data inferred from in-situ satellite measurements was harder and more time-consuming than expected.

It was realized that some satellite data is harder to find than other. On the one hand, it is a fact that many satellites offer to the public some of their processed data. On the other hand, some other data is either exclusively accessible in binary code (RAW) or not accessible at all.

During an extensive research, several potentially useful data was found from different missions:

- *AE* and *DE-2*: *NASA's* combination of *Atmosphere Explorer* satellites *AE-C, AE-D* and *AE-E* and *Dynamic Explorer 2* provide thermospheric measurements (i.e temperature and density) in the time ranges 1973-1981 and 1981-1983, respectively. These data sets can be found at *NASA's ATMOWEB* interface [59], which provides their numerical retrieval as well as its graphing. The instruments used for the retrieval of the data are specified, as well as what data they provided. It is noticeable the *AE* data have several data gaps of even several days due to duty cycle limitations.
- *GOCE*: this satellite is one of *ESA's* Earth observation missions. It studied Earth's gravity field from 2009 to 2013 and orbited at altitudes around 250 km, lower than any other satellite for this kind of mission [60]. *GOCE* data is accessible at the *ESA GOCE Virtual Archive* [61]. Its thermospheric density data is of interest in the scope of this project.
- *SWARM*: this mission was launched in 2013, consisting on a satellite constellation formed by three identical satellites: *Alpha* and *Bravo* orbiting at a mean altitude of 450 km and *Charlie* at 530 km. Its goal is to provide accurate geomagnetic field multi-point measurements and its temporal evolution, as well as electric field measurements [62]. These satellites are equipped with high-accuracy instruments such as accelerometers, magnometers and GPS.

ESA's SWARM data system [63] provides a lot of different information. It includes products produced per satellite, consisting of time series of relevant quantities observed along their orbits, corrected, calibrated and then converted to physical units for further engineering use. They also provide products benefited by the use of the whole constellation, being themospheric measurements one of them. The data found of most interest for the project was under the label *Level-2 Cat-1 Products*, under product type *DNSxPOD-2*, which holds time series measurements of neutral thermospheric density exclusively inferred from precise orbit determination data. A detailed description and location of these products can be found at the *SWARM Users-Data Access Manual* [64].

- *ISDC*: the *Information System and Data Center* within the *GFZ Data Center* [65] offers satellite orbit, Earth gravity field, geomagnetic and atmospheric data to the public. The *ISDC* collaborates in different projects such as *CHAMP*, *GRACE* and commonly known *GNSS*. The most relevant data for this project is the one provided by satellite *CHAMP*, which recorded gravity and magnetic field activity during its operating years (2000-2010) and it is used for space weather monitoring purposes.

Some other different organizations which hold satellite data were also searched, like *European Organization for the Exploitation of Meteorological Satellites (EUMESAT)* and *National Oceanic and Atmospheric Administration (NOAA)* for information on the *Meteorological Operational satellite, MetOp*.

Table 5 sums up the data found of interest for the project, determining the year-range each satellite provides as well as their orbital height.

Satellites	**Available data years**	**Orbital height [km]**	
SWARM	2014-2017	**A,B**	**C**
		450	530
GOCE	2009/11-2013/10	260	
CHAMP	2000-2010	460	
AE-C	1973-1978	mid 1975: 300 mid 1977: 400	
AE-D	1975-1976	elliptical orbit 150-3800	
AE-E	1975-1981	until mid 1977: orbital orbit 150-4300 then: 400	
DE-2	1981-1983	elliptical orbit 300-1000	

Table 5: Satellite data coverage

4.4.3 Test Dates Selection Process

The selected dates for testing are chosen based on *RSGA* recorded solar and geomagnetic activity within the **2010-2012** year range. Four different periods are identified, chronologically:

Period	Time	Solar Activity	Geomagnetic Activity
1	**April 2010**	Low	Moderate
2	**June 2010**	Low	Quiet
3	**November 2011**	Elevated	Quiet
4	**March 2012**	Moderate	Moderate

Table 6: Four Different Activity Periods

Then, model results are to be compared only to ***GOCE*** data. The aim of the present section is to explain what factors and how they affected this decision concerning model implementation. The complete date set with corresponding values of solar and geomagnetic activity is given in Table 13.

Online modelling presents an unfortunate constraint; the time-range of its modelling capabilities is limited, as specified in Table 7.

Model	Date Range [DD/MM/YYYY]
NRLMSIS-00	14/02/1960 - 17/04/2017
DTM-2013	01/01/1972 - 31/08/2012

Table 7: Online models' date constraints

This reduces the capability of the comparative analysis. Due to *DTM's* constraint being the most restricting, the year-range that can be analyzed is narrowed down to 1972-2012. This limiting factor leaves out *SWARM* data (2014-2017) for the comparative analysis. As it is too time-consuming to analyze the whole 1972-2012 year range, it is decided to evaluate a few time periods with high and low solar activity, based on $F_{10.7}$ and Ap recorded values.

Solar cycle 24 is the solar cycle in progress, which began in December 2008 and it is currently reaching its end, lasting about 10 years [66]. Then, the results belonging to *solar cycle 24* dates can be compared to *GOCE* and *CHAMP* data, following Table 8. In the same way, *solar cycle 23* key dates could be tested and compared to *CHAMP* data.

Satellites	**Available data years**	**Solar Cycle**				
		20 (1964-1976)	**21 (1976-1986)**	**22 (1986-1996)**	**23 (1996-2008)**	**24 (2008-present)**
GOCE	2009/11-2013/10					X
CHAMP	2000-2010				X	X
AE-C	1973-1978	X	X			
AE-D	1975-1976	X	X			
AE-E	1975-1981	X	X			
DE-2	1981-1983		X			

Table 8: Satellite data correspondence to solar cycles

To identify periods of more active solar activity, the $F_{10.7}$ provided by *RSGA* is observed during the *solar cycle 24* within the 2009-2012 year range so that it agrees with *GOCE* data and online modeling capabilities. It is remarkable to say that this year range within *solar cycle 24* was not specially active, as it does show $F_{10.7} > 190$, which is classified as high activity.

It can be seen in Figure 15 how years 2009 and 2010 had much lower activity. As *solar cycle 24* began in 2008, these years belong to the solar minimum. Up to September, it is observed how activity in 2011 is noticeable lower than in 2012. There is an exception in November 2011, where its activity is higher than in 2012. After September, activity in 2011 is higher than in 2012. The end of 2012 was of low activity, it should have constantly increased as mid-cycle approaches and so does the solar maximum.

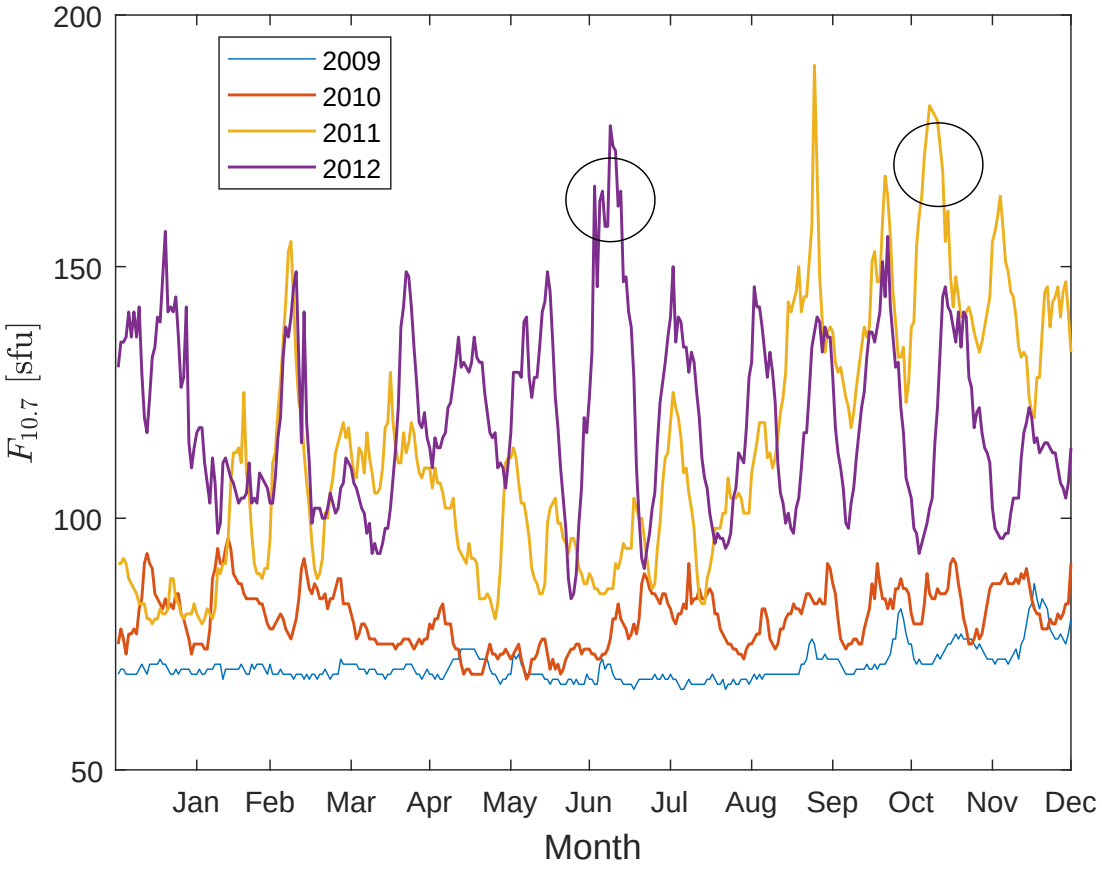

Figure 15: $F_{10.7}$ Index Comparison

The two more remarkable peaks of $F_{10.7}$ activity are pointed out in Figure 15 and represented in Figure 16 for a closer look. These correspond to November 2011 and July 2012. The highest $F_{10.7}$ indices are those for early November 2011, as specified in Table 9. It is noticeable that 2011/11/10, with $F_{10.7} = 179$ and $Ap = 3$ is skipped since *GOCE* data has a gap on that day. Also, in this table the corresponding Ap values are shown. Based on Table 2, it can be concluded that this period corresponds to elevated solar activity and quiet geomagnetic activity.

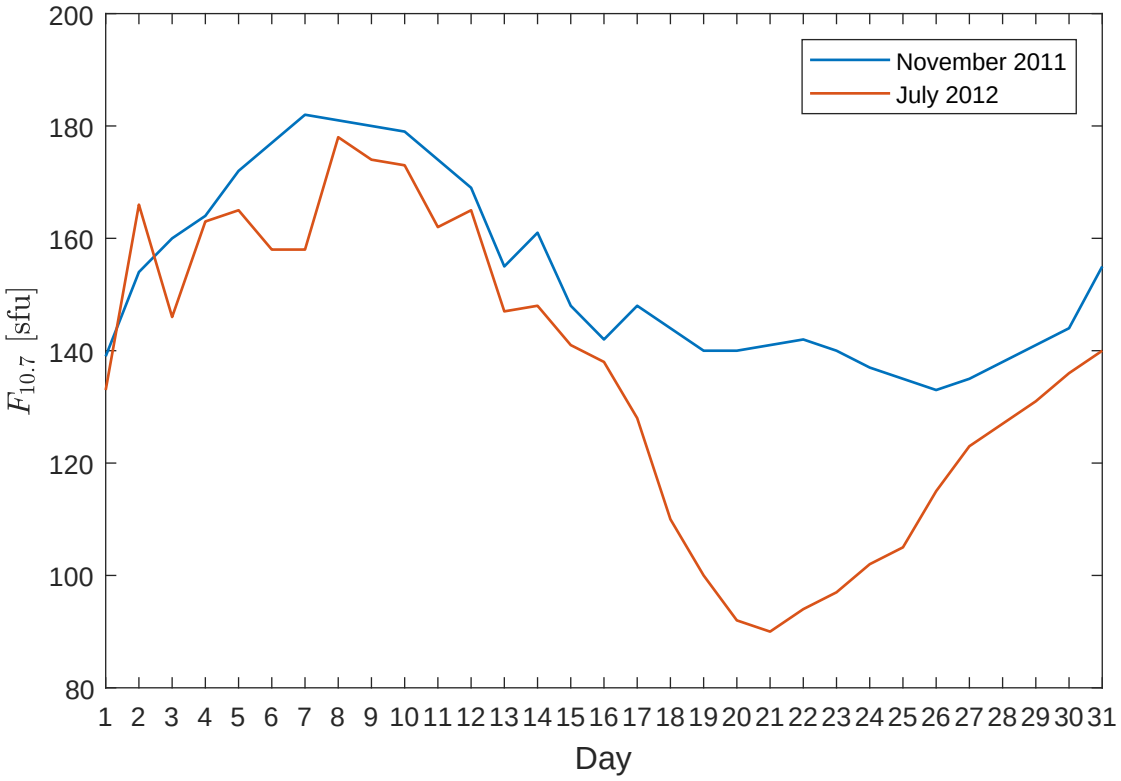

Figure 16: Most Active periods $F_{10.7}$ Index Comparison

Date [YYYY/MM/DD]	$F_{10.7}$	Ap
2011/11/04	164	4
2011/11/05	172	4
2011/11/06	177	3
2011/11/07	182	5
2011/11/08	181	6
2011/11/09	180	2
2011/11/11	174	4
2011/11/12	169	3
2011/11/13	155	2
2011/11/14	161	2

Table 9: Elevated Solar Activity and Quiet Geomagnetic Activity Period

As far as geomagnetic activity is concerned, the historical records on Ap values provided by *RSGA* are examined in the same 2009-2012 year range. Figure 17

shows how geomagnetic activity behaves very differently from day to day, as it has peaks of different magnitude.

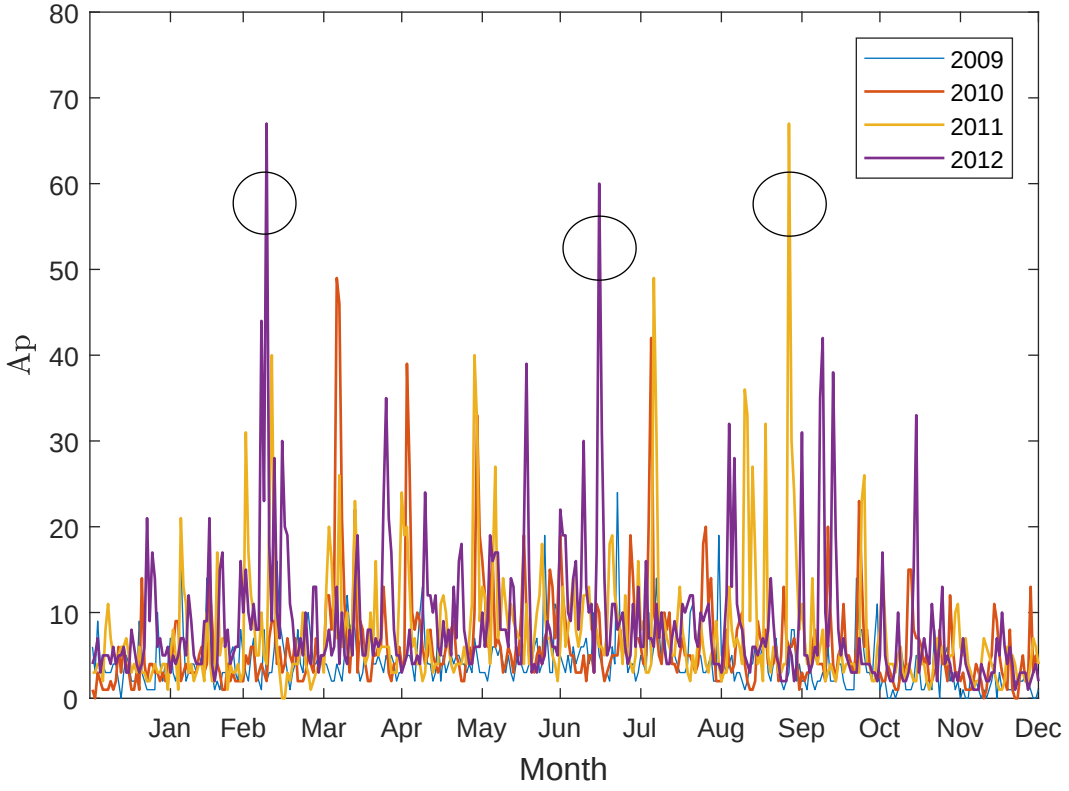

Figure 17: *Ap* Index Comparison

The three areas marked in Figure 17 corresponding to September 2011, March and July 2012 are given a closer look in Figure 18. The few consecutive high *Ap* correspond to punctual geomagnetic storms, which as it is seen, last a few days. Out of these three large peaks, March 2012 could be said to have had a few consecutive days of higher activity than the others. Due to a *GOCE* data gap from the 5^{th} to the 8^{th}, the following days to the geomagnetic storm of the 9^{th} are chosen for testing. Table 10 shows the *Ap* values and the corresponding solar activity indices, which in agreement with Table 2, it can be said that this period corresponds to moderate solar activity and moderate geomagnetic activity.

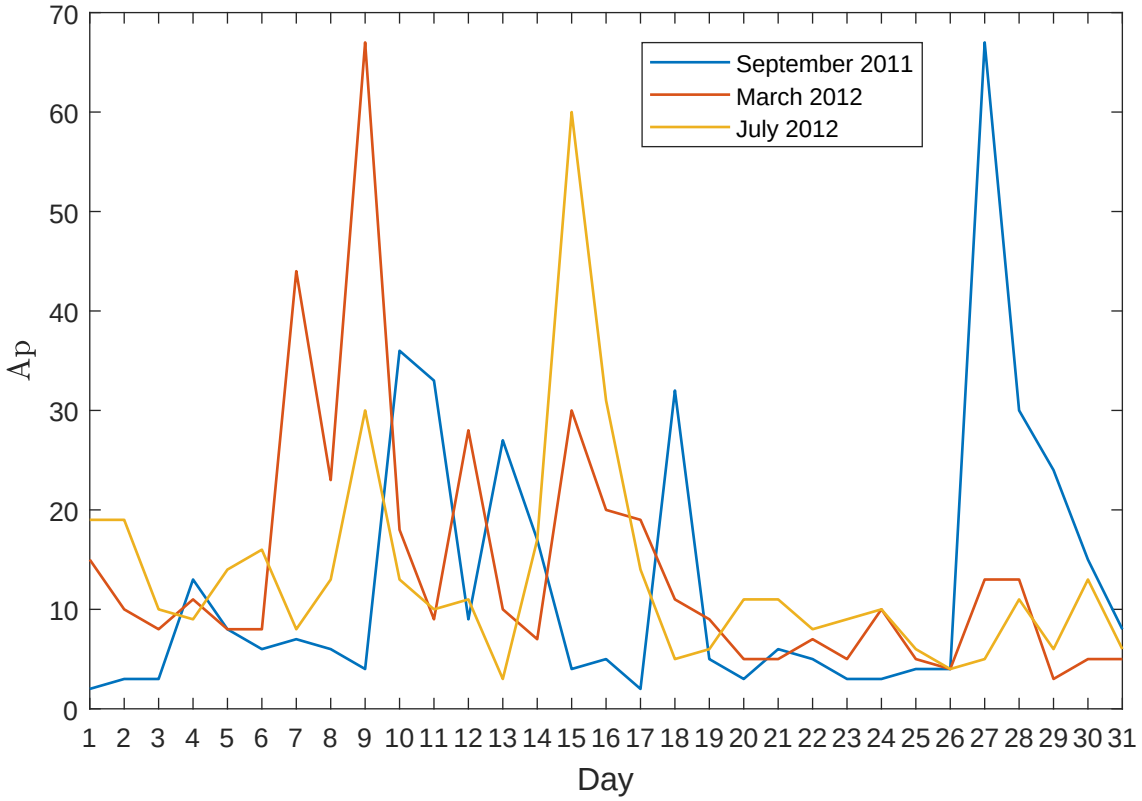

Figure 18: Most Active periods *Ap* Index Comparison

Date [YYYY/MM/DD]	$F_{10.7}$	*Ap*
2012/03/04	120	11
2012/03/09	146	67
2012/03/10	149	18
2012/03/11	131	9
2012/03/12	115	28
2012/03/13	141	10
2012/03/14	119	7
2012/03/16	99	20
2012/03/17	102	19
2012/03/18	102	11

Table 10: Moderate Solar Activity and Moderate Geomagnetic Activity Period

On the same line as the $F_{10.7}$ index, 2009 and 2010 were quieter years. Therefore, to study a range of dates where solar and geomagnetic activity were low according to

the criteria stated in Table 2, 10 days in early-mid June 2010 are chosen, see Table 11.

Date [YYYY/MM/DD]	$F_{10.7}$	Ap
2010/06/05	70	6
2010/06/06	68	7
2010/06/07	69	6
2010/06/08	72	3
2010/06/09	72	4
2010/06/10	73	6
2010/06/11	75	5
2010/06/12	76	3
2010/06/13	76	6
2010/06/14	73	5

Table 11: Low Solar Activity and Quiet Geomagnetic Activity Period

The last period of interest observed is in April 2010, which presented low solar activity during a moderate activity geomagnetic storm, see Table 12.

Date [YYYY/MM/DD]	$F_{10.7}$	Ap
2010/04/01	79	12
2010/04/02	76	12
2010/04/03	77	8
2010/04/04	79	13
2010/04/05	79	49
2010/04/06	78	46
2010/04/07	76	21
2010/04/08	76	11
2010/04/09	76	6
2010/04/10	75	3

Table 12: Low Solar Activity and Moderate Geomagnetic Activity Period

Finally, the selected dates for testing and to be compared to *GOCE* data are given in Table 13. The first five were selected for having low solar activity, the next five for exhibiting elevated EUV activity and the last three for being moderate and high geomagnetic activity days according to Table 2. It is to be noted that even though *CHAMP* data was found, it was written in binary language and lack of time for its decoding made it not possible to be used. Also, due to time-restriction and *GOCE* data being of high-resolution and more recent than *AE* and *DE* data, it was decided to focus the test bench on *GOCE* data.

Activity	**Test Case**	**Date [YYYY/MM/DD]**	$F_{10.7}$	Ap
Solar - Low Geomagnetic - Moderate	**1**	**2010/04/01**	79	12
	2	**2010/04/02**	76	12
	3	**2010/04/03**	77	8
	4	**2010/04/04**	79	13
	5	**2010/04/05**	79	49
	6	**2010/04/06**	78	46
	7	**2010/04/07**	76	21
	8	**2010/04/08**	76	11
	9	**2010/04/09**	76	6
	10	**2010/04/10**	75	3
Solar - Low Geomagnetic- Quiet	**11**	**2010/06/05**	70	6
	12	**2010/06/06**	68	7
	13	**2010/06/07**	69	6
	14	**2010/06/08**	72	3
	15	**2010/06/09**	72	4
	16	**2010/06/10**	73	6
	17	**2010/06/11**	75	5
	18	**2010/06/12**	76	3
	19	**2010/06/13**	76	6
	20	**2010/06/14**	73	5
Solar - Elevated Geomagnetic - Quiet	**21**	**2011/11/04**	164	4
	22	**2011/11/05**	172	4
	23	**2011/11/06**	177	3
	24	**2011/11/07**	182	5
	25	**2011/11/08**	181	6
	26	**2011/11/09**	180	2
	27	**2011/11/11**	174	4
	28	**2011/11/12**	169	3
	29	**2011/11/13**	155	2
	30	**2011/11/14**	161	2
Solar - Moderate Geomagnetic - Moderate	**31**	**2012/03/04**	120	11
	32	**2012/03/09**	146	67
	33	**2012/03/10**	149	18
	34	**2012/03/11**	131	9
	35	**2012/03/012**	115	28
	36	**2012/03/13**	141	10
	37	**2012/03/14**	119	7
	38	**2012/03/16**	99	20
	39	**2012/03/17**	102	19
	40	**2012/03/18**	102	11

Table 13: Selected Days for Testing based on *RSGA* Index Data

4.4.4 *GOCE* Data Analysis: Time and Coordinate Input Selection

Besides the being modeling year-range a limiting factor for the comparative analysis, so is the type of found satellite-measured data obtained. It was established to use *GOCE* data since it agrees with the modelling year-limit exhibited by the models.

The available *GOCE* data in the scope of the project is an extensive compilation of air density ($[kg/m^3]$ data from 2009/11 to 2013/10. The satellite orbited at an altitude around 240 km - 290 km and took measurements every 10 seconds. Therefore, this data provides air density measurements as a function of:

- Date: [YYYY/MM/DD]
- Time: [HH:MM:SS.SSS]
- Altitude [m]
- Geodetic Longitude [deg]
- Geodetic Latitude [deg]

As the dates have already been selected, it is now necessary to select input time and coordinates. For simplicity, the first parameter chosen is time at 12:00:00.000, and the rest of parameters will be those corresponding to the selected time based on the *GOCE* data (longitude and latitude are geodetic). Table 14 presents the complete set of input parameters that conform the test bench. Note that longitude is given in the [-180º - 180º] range and latitude in the [-90º - 90º] range. Any test bench specific modification for the models is further indicated in section *5 Implementation & Results*.

Test Case	**Date [YYYY/MM/DD]**	**Time [hh:mm:ss.sss]**	**Altitude [km]**	**Long. [deg]**	**Lat. [deg]**
1	**2010/04/01**	12:00:00.000	267.904	-84.950	-19.959
2	**2010/04/02**		275.194	101.582	-41.696
3	**2010/04/03**		269.954	98.681	-24.350
4	**2010/04/04**		266.213	96.497	-6.906
5	**2010/04/05**		265.00	94.472	10.567
6	**2010/04/06**		266.247	92.197	27.990
7	**2010/04/07**		268.901	89.019	45.311
8	**2010/04/08**		271.351	82.961	62.404
9	**2010/04/09**		272.053	61.161	78.481
10	**2010/04/10**		270.186	-44.626	79.706
11	**2010/06/05**		257.55	97.170	-4.544
12	**2010/06/06**		256.91	95.129	12.984
13	**2010/06/07**		259.80	92.771	30.460
14	**2010/06/08**		264.83	89.358	47.799
15	**2010/06/09**		270.11	82.438	64.853
16	**2010/06/10**		273.482	53.338	80.441
17	**2010/06/11**		274.166	-51.268	77.688
18	**2010/06/12**		272.084	-70.944	61.519
19	**2010/06/13**		268.303	-76.717	44.473
20	**2010/06/14**		264.514	-79.810	27.222
21	**2011/11/04**		262.576	-75.100	9.701
22	**2011/11/05**		265.573	-77.125	-7.813
23	**2011/11/06**		271.162	-79.331	-25.290
24	**2011/11/07**		278.023	-82.298	-42.661
25	**2011/11/08**		284.196	-87.626	-59.820
26	**2011/11/09**		287.755	-104.272	-76.237
27	**2011/11/11**		282.431	118.011	-65.568
28	**2011/11/12**		275.165	111.208	-47.931
29	**2011/11/13**		267.243	107.722	-30.172
30	**2011/11/14**		260.935	105.352	-12.481
31	**2012/03/04**		266.183	-67.473	48.202
32	**2012/03/09**		271.605	-80.946	-42.798
33	**2012/03/10**		278.916	-86.643	-60.668
34	**2012/03/11**		284.044	-105.963	-77.448
35	**2012/03/12**		285.589	148.272	-80.422
36	**2012/03/13**		283.399	119.326	-64.696
37	**2012/03/14**		278.283	112.493	-47.650
38	**2012/03/16**		266.709	106.771	-12.945
39	**2012/03/17**		263.676	104.745	4.504
40	**2012/03/18**		263.476	102.618	21.937

Table 14: Complete Test Bench of Non-optional Input Parameters

5 Implementation & Results

This section is dedicated to the explanation of how every model was used and what inputs were provided to them. It is important to point out that for the sake of constancy and simplicity, solar and geomagnetic indices are preferred to be the same for every model, if possible. It is a fact that databases from different observatories provide similar index values, usually varying ± 0.5.

The present *a posteriori* analysis is conducted as follows:

1. Required solar and magnetic activity indices for every test case are calculated and/or retrieved from a fit database.

2. These data are used as inputs in the model together with date, time and coordinate data from Table 14.

3. Atmospheric conditions are retrieved from the model.

4. Modelled conditions are compared to the real ones retrieved from *GOCE* satellite measurements.

5.1 *NRLMSISE-00*

First of all, input longitude coordinates need to be converted from [-180º - 180º] to [0º - 360º], as this model requires the longitude to be in the latter form. Instead of using the associated *NRLMSIS-00* database, it is decided to take $F_{10.7}$ and its 3-month average (which is the 81-day average centered on the input time) from the *JB-2008* database. Feeding the models with solar indices from the same database should help the comparative analysis to not be as affected by index differences. *Ap* values are those provided by the *RSGA*. Table 15 gives the complete set of inputs for the test. It is important to point that in the table, it is indicated that the $F_{10.7}$ values used in every test case are those from the previous day. It is also noticeable that they are very similar to those given by the *RSGA* in Table 13.

Test Case	Date [YYYY/MM/DD]	Longitude [0º - 360º]	F10 Prior day (JB-2008)	F10B (JB-2008)	Ap (RSGA)
1	**2010/04/01**	275.050	82.6	79.8	12
2	**2010/04/02**	101.582	80.9	79.7	12
3	**2010/04/03**	98.681	79.1	79.6	8
4	**2010/04/04**	96.497	76.1	79.4	13
5	**2010/04/05**	94.472	77.4	79.3	49
6	**2010/04/06**	92.197	78.7	79.2	46
7	**2010/04/07**	89.019	79.3	79	21
8	**2010/04/08**	82.961	77.7	78.9	11
9	**2010/04/09**	61.161	76.5	78.8	6
10	**2010/04/10**	315.374	75.9	78.7	3
11	**2010/06/05**	97.170	76.8	74.7	6
12	**2010/06/06**	95.129	74	74.7	7
13	**2010/06/07**	92.771	72.4	74.7	6
14	**2010/06/08**	89.358	68	74.7	3
15	**2010/06/09**	82.438	68.5	74.7	4
16	**2010/06/10**	53.338	71.9	74.7	6
17	**2010/06/11**	308.732	71.5	74.8	5
18	**2010/06/12**	289.056	72.9	75	3
19	**2010/06/13**	283.283	74.6	75	6
20	**2010/06/14**	280.190	76.2	75.1	5
21	**2011/11/04**	284.900	153.6	146	4
22	**2011/11/05**	282.875	160.4	145.3	4
23	**2011/11/06**	280.669	163.9	144.7	3
24	**2011/11/07**	277.702	171.9	144.4	5
25	**2011/11/08**	272.374	176.7	144.2	6
26	**2011/11/09**	255.728	182.1	144.1	2
27	**2011/11/11**	118.564	180.2	144	4
28	**2011/11/12**	111.208	178.6	144.1	3
29	**2011/11/13**	107.722	173.9	144.2	2
30	**2011/11/14**	105.352	168.8	144.4	2
31	**2012/03/04**	292.527	108.2	110.7	11
32	**2012/03/09**	279.054	135.7	108.8	67
33	**2012/03/10**	273.357	139.5	108.9	18
34	**2012/03/11**	254.037	145.5	109.2	9
35	**2012/03/12**	148.272	148.9	109.6	28
36	**2012/03/13**	119.326	131.2	110	10
37	**2012/03/14**	112.493	114.9	110.3	7
38	**2012/03/16**	106.771	118.8	110.9	20
39	**2012/03/17**	104.745	110.6	111.2	19
40	**2012/03/18**	102.618	98.5	111.4	11

Table 15: *NRLMSIS-00* Latitude, Solar and Geomagnetic Input Indices

5.2 *MET-07*

As it was mentioned before, an executable version of the FORTRAN code obtained from *NASA* was made, which was simple to use. Since *MET-07* requires the $F_{10.7}$ index and its 81-day average value centered on the input day, these two indices are also extracted from the *JB-2008* database. Therefore, the solar indices from Table 16 also correspond to the ones used for *MET-07* implementation, and the *Ap* indices correspond to those from *RSGA*. No further changes are made for this model with respect to Table 14.

5.3 *JB-2008*

The MATLAB test script for the implementation of the *JB-2008* model already has the necessary data to make its computations. The code is able to open and read Earth orientation parameters, space weather data and geomagnetic storm dT_c values.

In principle, the MATLAB code needs user-manually-provided year and day-of-year inputs to later calculate MJD to feed the *JB-2008* function. Since at first the day-of-year is unknown, the script has been altered so that date and time are provided in [YYYY/MM/DD] and [hh:mm:dd:ss.sss] formats, respectively. From these parameters, the day-of-year is computed and so is MJD. Based on the date and time provided, the program is able to locate and retrieve the solar and geomagnetic indices that correspond to them. The geographic longitude and latitude coordinates of the desired point of study are manually provided and then, longitude is translated to *right ascension* in radians. Altitude also needs to be provided for output calculations.

Table 16 shows the numerical values of the indices used in every test case.

Test Case	Date	F10	F10B	S10	S10B	XM10	XM10B	Y10	Y10B	dT_c
1	**2010/04/01**	80.9	79.8	69	67.7	78.1	78.1	85.7	80.7	85
2	**2010/04/02**	79.1	79.7	65.7	67.7	77.3	77.3	76.1	80.7	74
3	**2010/04/03**	76.1	79.6	65.8	67.7	77.2	77.2	83.4	80.7	38
4	**2010/04/04**	77.4	79.4	66	67.6	77.7	77.7	79.9	80.7	74
5	**2010/04/05**	78.7	79.3	66.6	67.6	75.3	75.3	80.2	80.5	94
6	**2010/04/06**	79.3	79.2	67.1	67.5	73.6	73.6	74.3	80.4	148
7	**2010/04/07**	77.7	79	66.9	67.4	75.7	75.7	73	80.2	60
8	**2010/04/08**	76.5	78.9	66.6	67.4	75.5	75.5	79.8	80.1	60
9	**2010/04/09**	75.9	78.8	66.2	67.3	78.6	78.6	77.7	79.9	60
10	**2010/04/10**	76.3	78.7	66.4	67.3	79.5	79.5	80.8	79.7	31
11	**2010/06/05**	74	74.7	64.1	68.1	76.5	75.3	82.1	81.6	38
12	**2010/06/06**	72.4	74.7	63.1	68.2	74.4	75.4	84.7	81.7	38
13	**2010/06/07**	68	74.7	60.9	68.4	75.9	75.5	83	81.9	31
14	**2010/06/08**	68.5	74.7	60.9	68.5	74.1	75.6	82.1	82	17
15	**2010/06/09**	71.9	74.7	62	68.6	70.4	75.6	81.8	82.2	24
16	**2010/06/10**	71.5	74.7	64.3	68.8	69.7	69.7	80.2	82.3	50
17	**2010/06/11**	72.9	74.8	64.6	68.9	69.1	69.1	78.6	82.4	38
18	**2010/06/12**	74.6	75	66.5	68.9	69.8	69.8	79	82.6	17
19	**2010/06/13**	76.2	75	69.4	69	70	70	80.4	82.8	44
20	**2010/06/14**	76.3	75.1	70.1	69.1	71.9	71.9	79.9	82.9	31
21	**2011/11/04**	160.4	146	173.2	171.1	114	114	141.8	143.1	0
22	**2011/11/05**	163.9	145.3	174.5	171.1	128.2	128.2	146.9	143.1	38
23	**2011/11/06**	171.9	144.7	178.3	171.1	129.7	136.1	145.9	143	0
24	**2011/11/07**	176.7	144.4	183.2	171.1	134.7	136.1	149	142.9	44
25	**2011/11/08**	182.1	144.2	185.2	171.2	142.3	136.2	147.6	142.9	60
26	**2011/11/09**	181	144.1	187.2	171.4	150.7	136.3	149.2	142.6	0
27	**2011/11/11**	178.6	144	198	171.7	162.7	136.6	148.9	142.2	44
28	**2011/11/12**	173.9	144.1	198	171.8	165.7	165.7	150.4	142.2	0
29	**2011/11/13**	168.8	144.2	196.8	171.9	166.1	166.1	152.2	142.3	0
30	**2011/11/14**	155.3	144.4	197.6	172	162.7	162.7	154.5	142.3	17
31	**2012/03/04**	116.4	110.7	103.7	103.5	114.9	114.9	120.4	120.2	85
32	**2012/03/09**	139.5	108.8	105.1	102.6	128.2	111.2	130.3	118.2	271
33	**2012/03/10**	145.5	108.9	110.5	102.6	110.8	110.8	129.1	118	135
34	**2012/03/11**	148.9	109.2	111.3	102.7	112.9	112.9	129	117.9	44
35	**2012/03/12**	131.2	109.6	106.7	102.7	116.1	116.1	129.4	117.7	44
36	**2012/03/13**	114.9	110	106.8	102.8	115.3	115.3	132.6	117.7	94
37	**2012/03/14**	140.7	110.3	110	102.9	115.1	115.1	133.4	117.7	50
38	**2012/03/16**	110.6	110.9	104.4	103	111.1	111.1	126.4	117.8	94
39	**2012/03/17**	98.5	111.2	100.8	103.2	109	109	124.3	118	115
40	**2012/03/18**	102.4	111.4	97.2	103.3	106.5	106.5	127.2	118.2	105

Table 16: *JB-2008* Input Space Weather Indices

5.4 *DTM-2013*

Due to input precision of the online interface, the tests are run with modified values of altitude, longitude and latitude, since the model admits precision to unity (not decimals). Table 17 shows the actual inputs rounded up from the values given in Table 14.

Test Case	**Date [YYYY/MM/DD]**	**Altitude [km]**	**Long. [deg]**	**Lat. [deg]**
1	**2010/04/01**	268	-85	-20
2	**2010/04/02**	275	102	-42
3	**2010/04/03**	270	99	-24
4	**2010/04/04**	266	96	-7
5	**2010/04/05**	265	94	11
6	**2010/04/06**	266	92	28
7	**2010/04/07**	269	89	45
8	**2010/04/08**	271	83	62
9	**2010/04/09**	272	61	78
10	**2010/04/10**	270	-45	80
11	**2010/06/05**	258	97	-4
12	**2010/06/06**	257	95	13
13	**2010/06/07**	260	93	30
14	**2010/06/08**	265	89	48
15	**2010/06/09**	270	82	65
16	**2010/06/10**	273	53	80
17	**2010/06/11**	274	-51	78
18	**2010/06/12**	272	-71	61
19	**2010/06/13**	268	-77	44
20	**2010/06/14**	264	-80	27
21	**2011/11/04**	263	-75	10
22	**2011/11/05**	266	-77	-8
23	**2011/11/06**	271	-79	-25
24	**2011/11/07**	278	-82	-43
25	**2011/11/08**	284	-88	-60
26	**2011/11/09**	288	-104	-76
27	**2011/11/11**	282	118	-66
28	**2011/11/12**	275	111	-48
29	**2011/11/13**	267	108	-30
30	**2011/11/14**	261	105	-12
31	**2012/03/04**	266	-67	48
32	**2012/03/09**	272	-81	-43
33	**2012/03/10**	279	-87	-61
34	**2012/03/11**	284	-106	-77
35	**2012/03/12**	286	148	-80
36	**2012/03/13**	283	119	-65
37	**2012/03/14**	278	112	-48
38	**2012/03/16**	267	107	-13
39	**2012/03/17**	264	105	4
40	**2012/03/18**	263	103	22

Table 17: *DTM-2013* Test Bench Date, Time and Coordinates Input Values

Since *Dr. Cefola* pointed that both F_{30} and $F_{10.7}$ are valid when running the model, they are used. F_{30} values re-scaled to $F_{10.7}$, akp(1) and akp(3) were retrieved from the associated *DTM* database. Then, to keep it as similar to the other inputs as possible, the $F_{10.7}$ values are the same ones used for *MET-07* and *JB-2008*, retrieved from the database associated to *JB-2008*. As it is not easy to compute the Kp values, the same ones as with F_{30} are used. Table 18 shows the values used.

Test Case	**Date [YYYY/MM/DD]**	**f (from F_{30})**	**fbar (from F_{30})**		**f ($F_{10.7}$ from JB-2008)**	**fbar ($F_{10.7}$ from JB-2008)**		**akp(1)**	**akp(3)**
1	**2010/04/01**	80.7	80.7		80.9	79.8		1.728	2.128
2	**2010/04/02**	78.4	85.5		79.1	79.7		3.405	2.907
3	**2010/04/03**	77.6	85.3		76.1	79.6		1.099	2.416
4	**2010/04/04**	78.4	85.2		77.4	79.4		1.506	2.712
5	**2010/04/05**	79.2	85.0		78.7	79.3		6.215	3.615
6	**2010/04/06**	80.7	84.9		79.3	79.2		4.383	4.540
7	**2010/04/07**	80.7	84.9		77.7	79		3.952	4.100
8	**2010/04/08**	80.0	84.8		76.5	78.9		2.694	3.223
9	**2010/04/09**	80.0	84.7		75.9	78.8		1.396	2.224
10	**2010/04/10**	80.0	84.6		76.3	78.7		0.429	1.451
11	**2010/06/05**	74.5	79.0		74	74.7		0.762	1.806
12	**2010/06/06**	72.2	78.8		72.4	74.7		1.616	1.602
13	**2010/06/07**	70.6	78.6		68	74.7		1.506	1.540
14	**2010/06/08**	69.9	78.3		68.5	74.7		0.594	1.078
15	**2010/06/09**	72.2	78.2		71.9	74.7		0.932	0.720
16	**2010/06/10**	74.5	78.0		71.5	74.7		2.066	1.513
17	**2010/06/11**	76.1	78.0		72.9	74.8		1.264	1.212
18	**2010/06/12**	79.2	78.0		74.6	75		0.236	0.635
19	**2010/06/13**	80.7	77.9		76.2	75		2.066	1.068
20	**2010/06/14**	80.7	77.7		76.3	75.1		1.728	1.485
21	**2011/11/04**	156.9	132.5		160.4	146		1.396	0.698
22	**2011/11/05**	162.3	133.4		163.9	145.3		0.762	1.424
23	**2011/11/06**	168.5	134.4		171.9	144.7		0.932	0.563
24	**2011/11/07**	176.3	135.4		176.7	144.4		1.396	1.458
25	**2011/11/08**	183.3	136.5		182.1	144.2		1.955	1.948
26	**2011/11/09**	188.7	137.6		181	144.1		0.762	1.389
27	**2011/11/11**	193.4	139.8		178.6	144		1.728	1.316
28	**2011/11/12**	187.2	140.6		173.9	144.1		1.955	0.826
29	**2011/11/13**	179.4	141.4		168.8	144.2		1.264	0.911
30	**2011/11/14**	172.4	142.2		155.3	144.4		0.762	0.666
31	**2012/03/04**	117.3	131.9		116.4	110.7		2.807	2.642
32	**2012/03/09**	124.3	130.8		139.5	108.8		6.775	5.257
33	**2012/03/10**	125.8	130.5		145.5	108.9		3.123	4.391
34	**2012/03/11**	127.4	130.3		148.9	109.2		2.176	2.313
35	**2012/03/12**	126.6	130.0		131.2	109.6		5.575	3.002
36	**2012/03/13**	121.9	129.7		114.9	110		1.841	3.663
37	**2012/03/14**	122.7	129.4		140.7	110.3		1.616	1.969
38	**2012/03/16**	115.7	128.4		110.6	110.9		4.350	4.362
39	**2012/03/17**	112.6	127.9		98.5	111.2		3.170	3.819
40	**2012/03/18**	113.4	127.4		102.4	111.4		2.751	3.364

Table 18: *DTM-2013* Input Solar and Geomagnetic Indices

The *DTM-2013* "single call" function is used to obtain air density values for the test cases. Figures 19 and 20 represent the values obtained using the different solar fluxes in the four periods, as well as the error associated to each calculation. This error varies from approximately 3% to 10% for both fluxes.

Figure 19 represents the periods of low solar and moderate geomagnetic activity (period 1) and low solar and quiet geomagnetic activity (period 2), where it is clear that air density values calculated using $F_{10.7}$ index are slightly closer to the target values than those calculated with the F_{30} index. Since geomagnetic activity indices are kept the same for both evaluations, solar activity is responsible for this air density difference; the higher the solar activity, the more the thermosphere heats up, the denser the layers found at the same height due to the before-mentioned "puff-up" effect. Therefore, since F_{30} and its 81-day centered average values are higher than those given by the $F_{10.7}$ flux, see Table 18, they provide higher density.

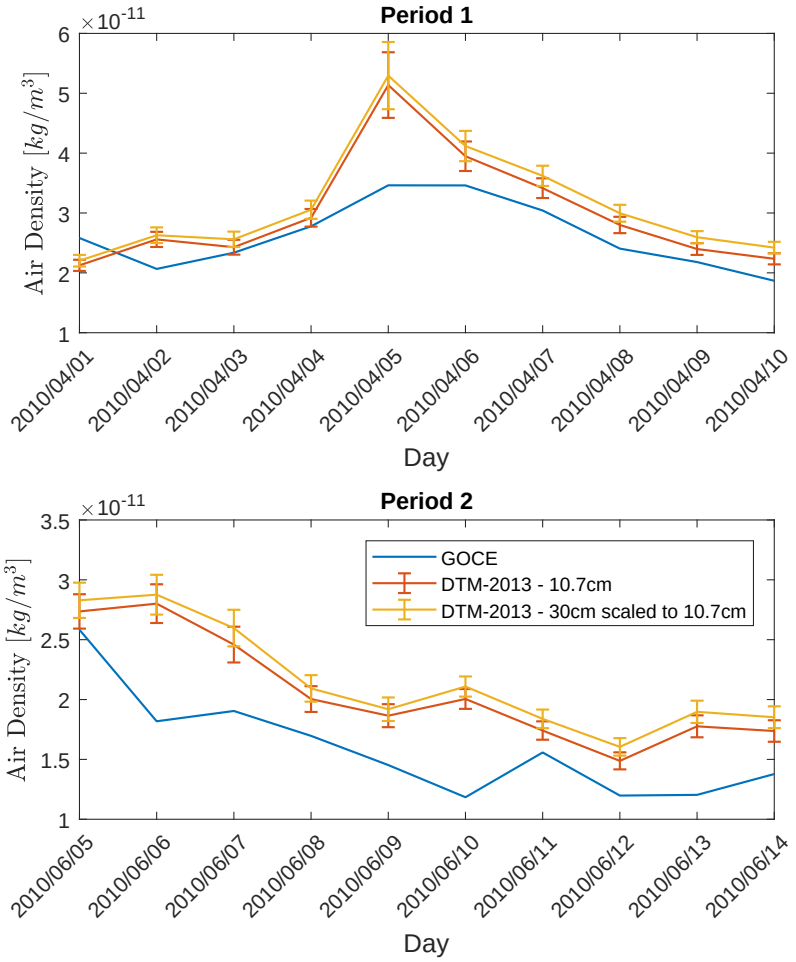

Figure 19: *DTM-2013* Solar 30cm and 10.7cm Flux Comparison, Periods 1 and 2

The same conclusion is reached from Figure 20, although it is not as clear. For the elevated solar and quiet geomagnetic activity period (period 3), F_{30} provides slightly better results up to 2011/11/09. F_{30} indices and its corresponding 81-day centered averages are mostly lower than those of $F_{10.7}$ up to 2011/11/09, and therefore, they provide lower density. When $F_{10.7}$ values are smaller, they provide better results, and this happens in the 77.5% of the cases tested.

In the contrary to what was expected, it is decided to use the air density results provided by the $F_{10.7}$ solar index for further comparisons. Also, by doing so, the same solar index is used for all the models, which keeps the analysis less biased.

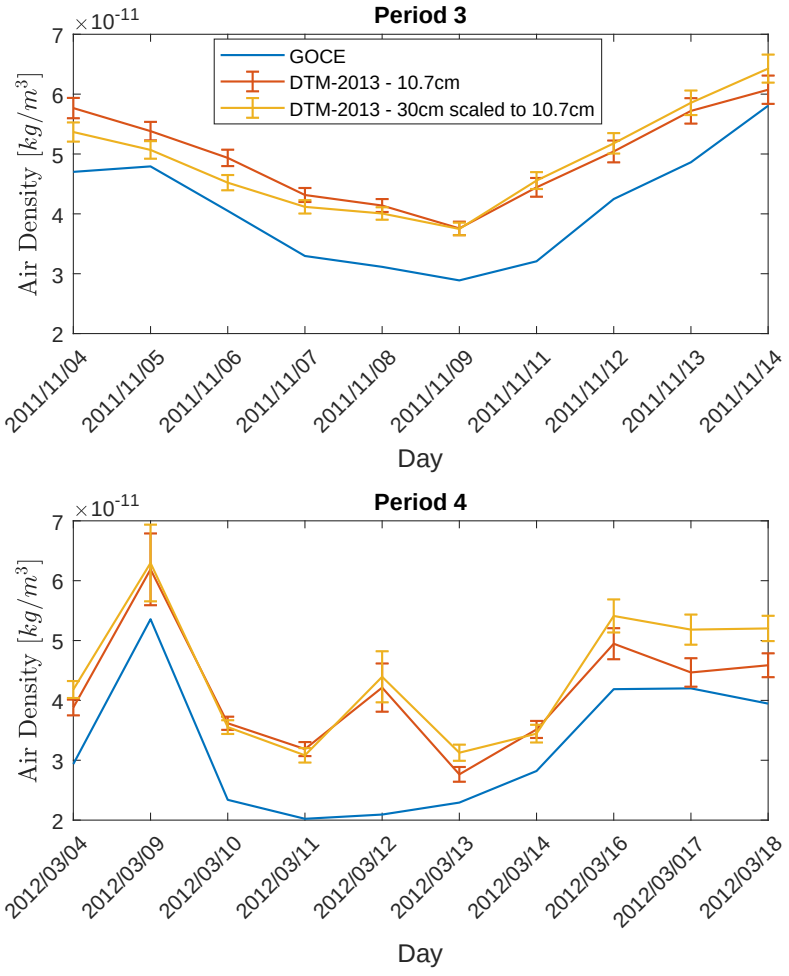

Figure 20: *DTM-2013* Solar 30cm and 10.7cm Flux Comparison, Periods 3 and 4

Even though the following results are not used in the main comparison of the models, it was considered interesting to see what the "global density distribution at a height" functionality provides.

The global density distribution of test cases 11 and 32, at an altitude of 256 km and with their corresponding $F_{10.7}$ solar and geomagnetic values from Table 18 are represented in Figures 21 and 22, respectively. Since both cases are evaluated at 256 km, it can be observed how density behaviour agrees with the thermosphere puff-up phenomenon explained in section *3.1.1 Satellite Drag Data*; air density is higher in test case 32 due to the increased solar and geomagnetic activities.

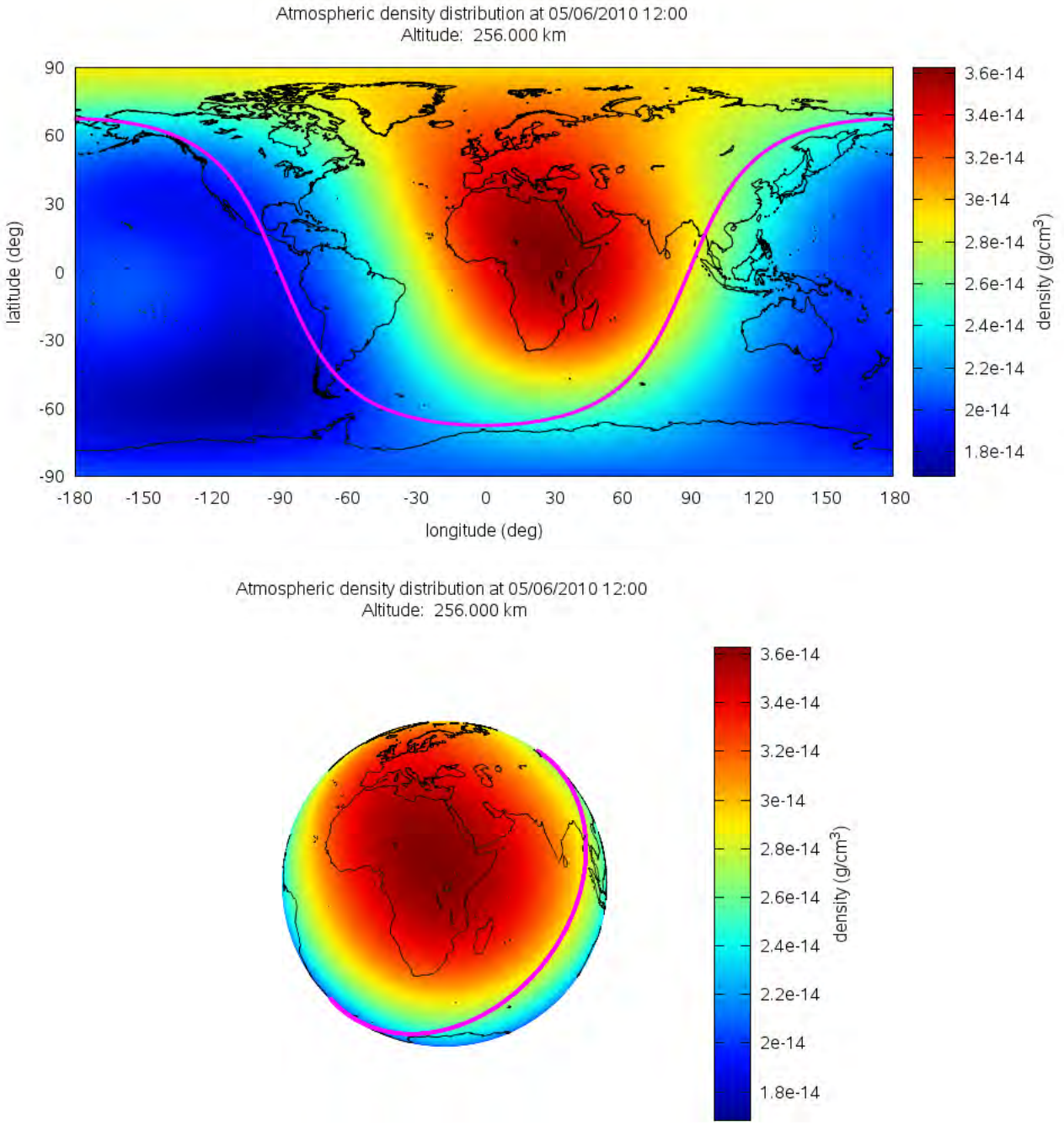

Figure 21: Test Case 11 Global Density Distribution at 256 km

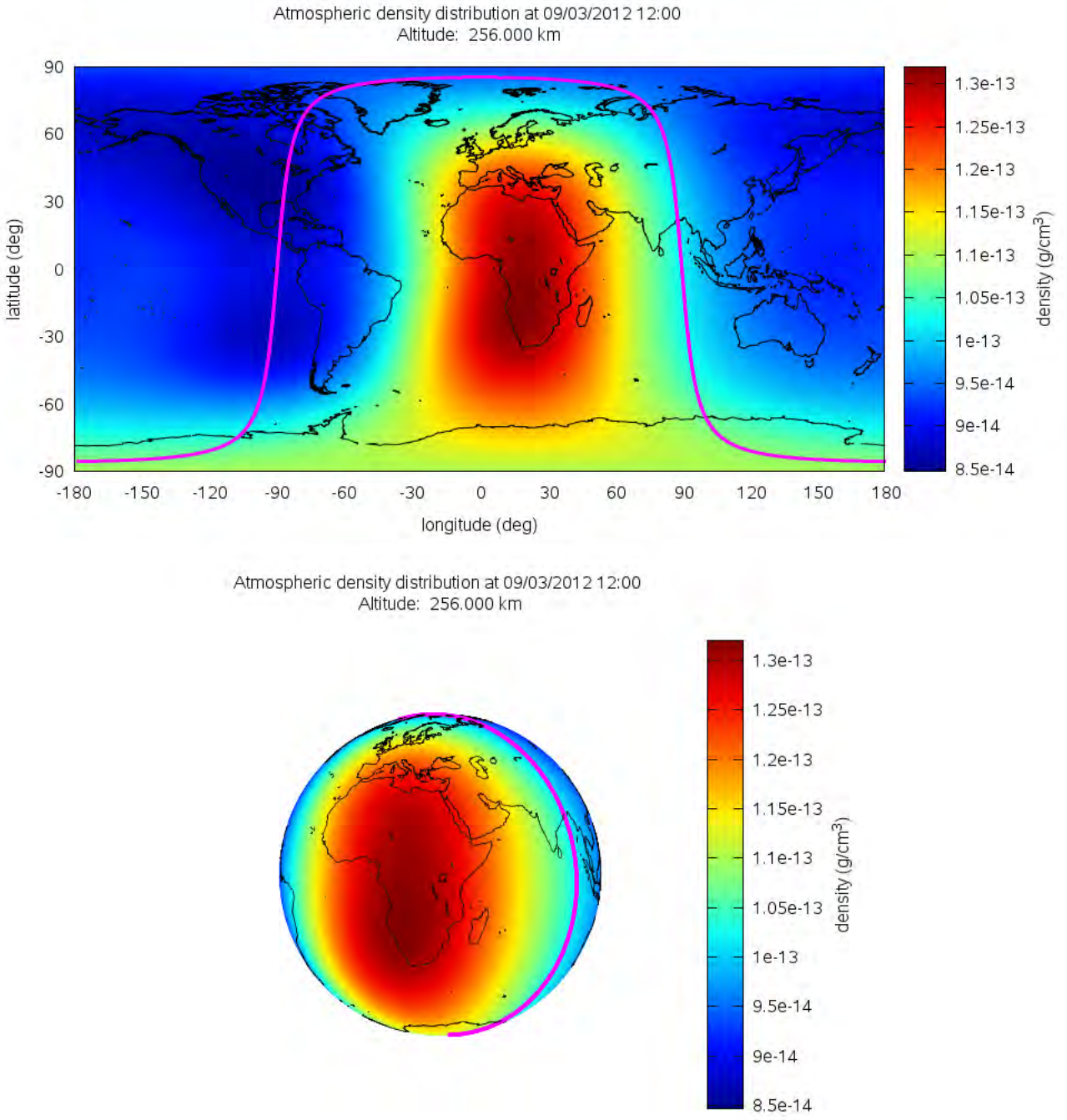

Figure 22: Test Case 32 Global Density Distribution at 256 km

5.5 Air Density Models and *GOCE* Data Comparison

The following subsections are dedicated to the independent analysis of every period, aiming to identify the model with higher performance or if such performance is biased to different combinations of solar and geomagnetic activity.

The density ratios presented in the study are computed as observed/calculated (*GOCE*/model) data, therefore:

- ratio < 1 : model overestimates actual data.
- ratio > 1 : model underestimates actual data.

To conclude the results are accurate and the models to be of good performance, a deviance of $\pm 5\%$ with respect to actual data is considered acceptable, which is translated to calculated data being in the 0.95-1.05 ratio range. This ratio is considered acceptable in several prior studies, such as *The contribution of GOCE densities to the semi-empirical thermosphere model DTM*, conducted by *Dr. Bruinsma* [67].

5.5.1 Period 1: Low Solar and Moderate Geomagnetic Activities

The results for period 1 shown in Figure 23 are quiet satisfactory. All the models seem to maintain their results between the 1 - 0.8 ratio, meaning their overestimation is less than the +25% with respect to *GOCE* data. *JB-2008* and *NRLMSIS-00* succeed to be within $\pm 5\%$ difference range, providing higher performance than the others.

On the other hand, while *MET-07* values seem to be stable at +25%, *DTM-2013* presents more peaks and stabilizes at the end of the period at approximately +16% (ratio = 0.86). The latter model also provides the result which falls the furthest from actual data, which happens on 2010/04/05 and whose ratio equals 0.674 (+48.36%).

It can be therefore concluded that for low solar and moderate geomagnetic activities, the most reliable models are *JB-2008* and *NRLMSIS-00*.

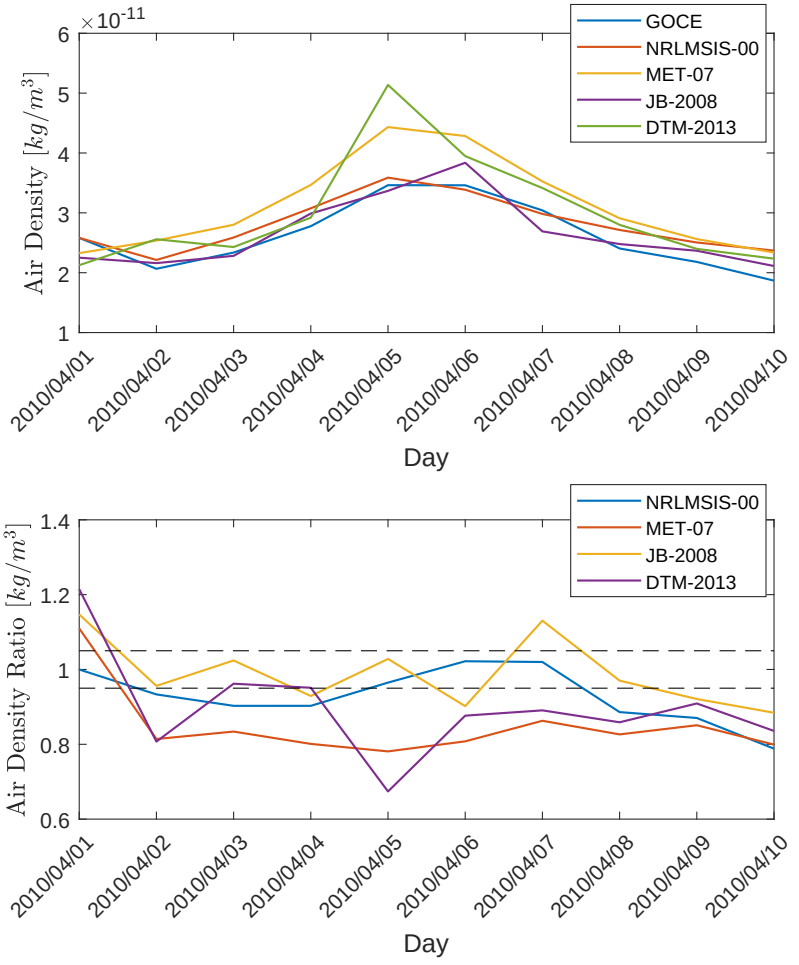

Figure 23: Period 1 Air Density Comparison

5.5.2 Period 2: Low Solar and Quiet Geomagnetic Activities

The results for period 2, presented in Figure 24, are not nearly as satisfactory as those obtained for period 1. The models' results differ considerably within the 0.85 - 0.55 ratio range, approximately 17% to 81% above actual data.

JB-2008 is the model that presents closer results to actual data, succeeding to provide two values in the 0.95 - 1.05 range. Nevertheless, the rest of the results fall within the 0.85 - 0.80 ratio range (+17% - +25%), overestimating the density by 51% on 2010/06/10 with respect to the real value.

In this case, *DTM-2013* offers better results than *NRLMSIS-00*, since the later gives approximately higher results in a 10% - 12% in comparison to the former. It is noticeable that *MET-07* has the lowest performance, showing a difference as high as +89% on 2010/06/06.

It can be stated that *JB-2008* has the highest performance out of the four models in this period, although its results are not as accurate as as for period 1.

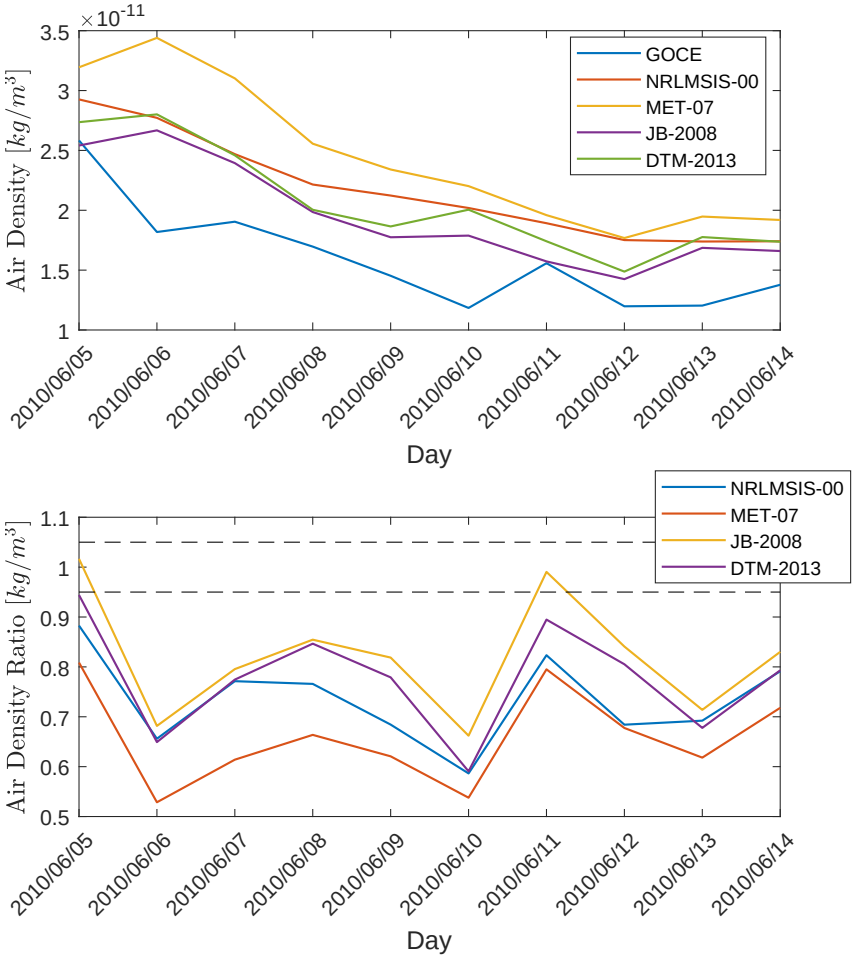

Figure 24: Period 2 Air Density Comparison

5.5.3 Period 3: Elevated Solar and Quiet Geomagnetic Activities

In the contrary to the previous studied periods, it is remarkable to observe that *JB-2008* is the model who falls further away from the actual *GOCE* data, as shown in Figure 25. The air density value provided for 2011/11/11 has a deviation of +74.3% with respect to the actual value.

The other three maintain their results in the 0.9-0.7 ratio range, which is translated to an overestimation between the 11% to 42%. The *MET-07* does slightly better than the *JB-2008*, although its results are still in the 0.85-0.7 ratio range.

DTM-2013 offers more accurate results than the *NRLMSIS-00* at the immediate beginning of the period, being then *NRLMSIS-00* the one which falls closer to actual data, even providing an underestimated air density value for 2011/11/14 within the -5%.

It can be stated that *NRLMSIS-00* is the model of highest performance in this period, followed by *DTM-2013*, even though their results are not as good those provided by *JB-2008* in period 1.

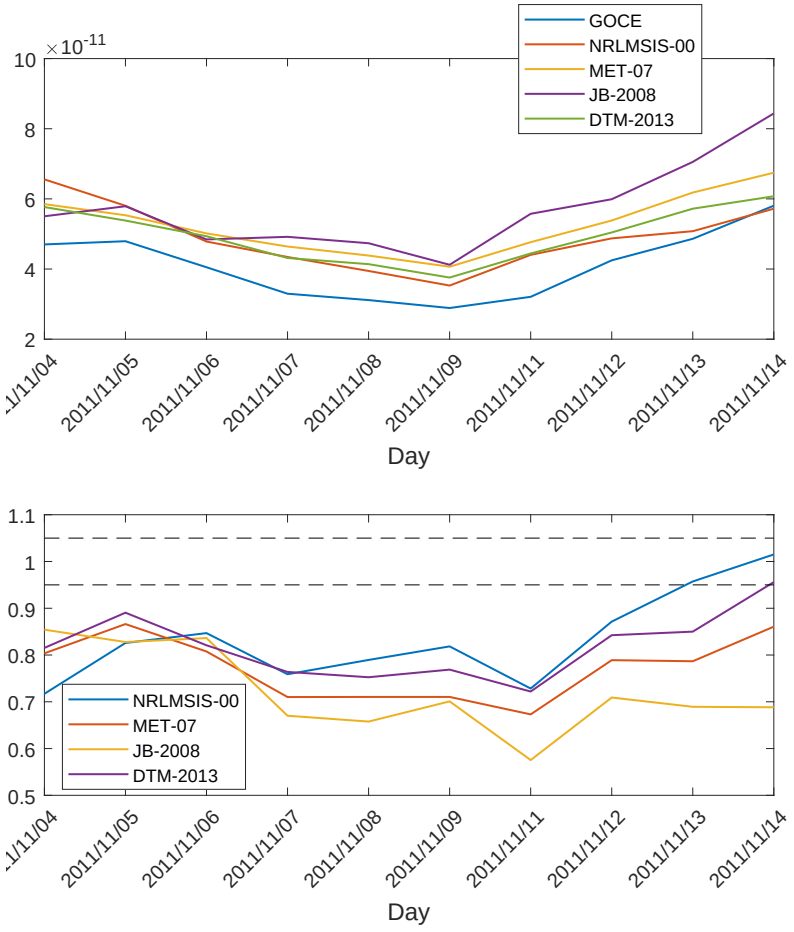

Figure 25: Period 3 Air Density Comparison

5.5.4 Period 4: Moderate Solar and Moderate Geomagnetic Activities

More satisfactory results seem to have been obtained for this period. It is remarkable to point out that on 2012/03/09, *JB-2008* succeeds to provide an underestimated value of -4%, whereas *MET-07* and *NRLMSIS-00* underestimation falls to ratios equal to 1.167 and 1.278, translated to a decrease of the 14.3% and 21.7%, respectively. On the other hand, *DTM-2013* provides an overestimated value of +15.6%.

For the rest of the period, *MET-07* gives rather better results than *DTM-2013*, with the exception at the immediate end of the period where the latter model almost reaches +5% difference with *GOCE* data.

NRLMSIS-00 provides very good results at approximately +5% with respect to actual data at the end of the period. Meanwhile, the values given by *JB-2008* are slightly higher and do not fall within the desired ±5%. Consequently, it is stated that *NRLMSIS-00* offers the best results in this period.

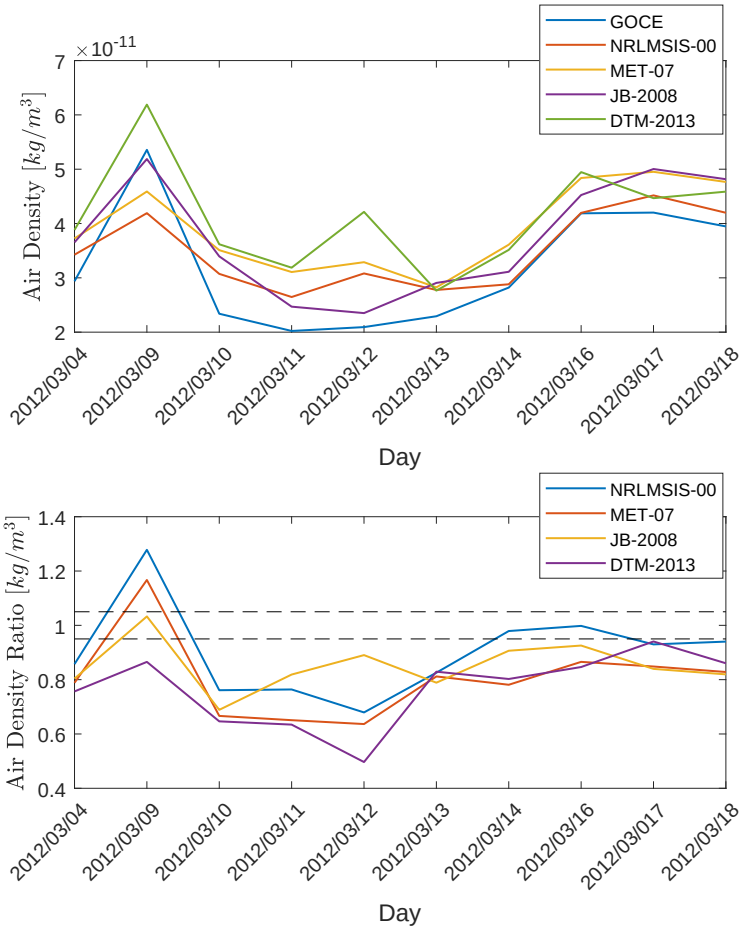

Figure 26: Period 4 Air Density Comparison

As the four periods have been examined, Table 19 sums up their ranking based on performance. They are ranked from 1 to 4, being 1 the model with highest performance and 4, with lowest. When two models are determined to have similar performances, they are ranked with the same number.

Period	Activity	NRLMSIS-00	MET-07	JB-2008	DTM-2013
1	**Solar - Low Geomagnetic - Moderate**	1	2	1	2
2	**Solar - Low Geomagnetic - Quiet**	3	4	1	2
3	**Solar - Elevated Geomagnetic - Quiet**	1	4	3	2
4	**Solar - Moderate Geomagnetic - Moderate**	1	3	2	4

Table 19: Models' Performance Ranking in the Different Periods

It is important to point out that the results retrieved from the analysis are limited to *GOCE* density data at 260 km - 290 km over specific period from 2010 to 2012, so these results may not apply to the whole thermosphere.

It can be seen that *NRLMSIS-00* and *JB-2008* are the two models with best overall performances. Their performance in the first period is outstanding, as they succeed to provide values within the desired $\pm 5\%$ deviance range. It appears that the *NRLMSIS-00* density function based on empirical data collected is well characterized as it succeeds to deliver accurate results. As for *JB-2008*, this could be due to the introduction of new space weather indexes which accounts for a more accurate modeling of solar heating and density changes during geomagnetic storms, like the Dst index. For the rest of the periods, the results are not as satisfactory. *JB-2008* does better in period 2, but its capability is reduced in period 3. *NRLMSIS-00* succeeds to give quiet good results in periods 3 and 4.

As far as *DTM-2013* is concerned, it seems to often exhibit pronounced peaked results when the other models do not, as in period 4. In contrary to what was expected from previous research on this model, F_{30} solar index did not provide better results than the $F_{10.7}$ index. This difference could be due to the fact that different databases were used for each of them, and it was decided to continue the study with the $F_{10.7}$ values provided by *JB-2008*, to try and keep the models' inputs as similar as possible.

Finally, *MET-07* seems to be the model which gives the least accurate results; it tends to overestimate air density in the highest percentage. This might appear as a shock since *MET-07* is widely used by *NASA*. The *MET-07* is a semi-empirical model which above 105 km integrates the diffusion equations to calculate density [14], and whose coefficients are obtained from satellite drag data. It could be the case where these coefficients are not very optimized for the height being analyzed, leading to a less-accurate determination of density. Also, data from different satellites could

have been used for its parametrization, so it might work better when compared to them.

6 Socio-economic Impact

A space mission budget depends on several parameters; manufacturing, launching, putting the satellite into service, to name a few. An estimation can be done as follows [68]:

- Manufacturing: overall, a typical weather satellite can end up costing $290 million, whereas a spy satellite can cost an extra $100 million. This high cost is linked to the high-technology equipment it carries: transponders, cameras, etc.
- Launching: depending on the vehicle used, launching can cost between $10 and $400 million. This cost varies depending on how much weight per dollar can be lift. Heavy-launch vehicles can be more cost-effective on this basis, for example, *Ariana 5G* rocket's lift-off costs $4 162/pound, whereas small launch rocket *Pegasus XL* costs $14 000/pound (for LEO orbits).
- Satellite bandwidth: satellites must pay up to $1.5 million per year to transmit their data.

The use of high-performing and reliable atmospheric models can have a positive impact in our economy, as well as in our society and environment, based on the following aspects.

Being able to accurately estimate air density is essential for atmospheric drag calculations, which lead to the orbital decay of LEO satellites. Due to such orbital decay, LEO satellites need to be constantly re-boosted to their appropriate orbits, mainly to avoid early re-entry to the atmosphere, which causes the complete destruction of the satellite. The constant re-boosting of the satellites is costly, since every orbit manoeuvre needs a certain amount of fuel, which is limited by fuel-tank capacity. The correct determination of air density would allow for a correct manoeuvre estimation, which would lead to avoid unnecessary manoeuvres, and consequently, to the optimization of fuel consumption which extends satellite lifetime. Extending the useful lifetime holds several advantages; the more the satellite lasts, the longer it can work on its mission, which could mean data retrieval covering a longer period of time. On top of this, the longer it lasts, the more amortized is its investment. In the long run, the longer a satellite works, the less satellites are needed to fill in their spot. At the same time, knowing the amount of fuel needed is required at early stages of the design process since it will affect its structure.

Furthermore, it is a fact that satellites are not meant to be repaired. In the design process, every aspect that could go wrong is considered and different scenarios are tested. Despite these efforts, satellite failures do happen and these man-made objects may temporarily become part of the so-called *space debris*, at least until their re-entry to Earth. When being large enough, it is possible that their falls can cause damages on Earth's surface, as the recent fall of the Chinese international

space station *Tiangong-1*, which was out of control and its 30-minute early re-entry happened at the southern Pacific Ocean [69]. Also, for example, it can happen that a part or fragment is dispatched, which can affect the normal operation of other satellites. The increased amount of *space debris* presents more collision risk for LEO satellites, which leads to the need for avoiding manoeuvres. The need for more manoeuvres increases the risk of running out fuel, which shortens the satellite's lifetime. Therefore, since atmospheric drag is used in orbit propagation models that are used to determine space object location and long-term predictions on *debris* environment for collision avoidance and re-entry predictions [37], accurate atmospheric models are essential.

7 Conclusions

7.1 Summary and Objectives Met

Atmospheric modeling has been on ongoing development and enhancement since the 1960s. Due to the fast growth of technology and demands within the aerospace industry, high-accuracy and high-performing models are needed for spacecraft design and on-orbit satellite operations. As it was said before, atmospheric drag provokes orbital decay which can represent the anticipated end of many LEO satellites. Therefore, a good estimation of air density is essential, so that satellites can at least last their whole expected useful lifetime or even more.

The present project has end up being more focused on scientific research than on model implementation due to the limited resources available. A satisfactory introduction to the dynamic behaviour of upper atmospheric layers has been carried out while examining the factors that alter them and how they are introduced in the models. Also, the different techniques used to retrieve empirical data are characterized.

Nevertheless, after an exhaustive research on current atmospheric models, the *NRLMSIS-00, MET-07, JB-2008* and *DTM-2013* were determined to be the global and permanent models of interest for implementation and testing. The different inputs required were examined, as well as where and in what format space weather indices are accessible to the public. After setting up a proper test bench based on different solar and geomagnetic activities, the main goal of the project, which was to find a model with high performance able to accurately represent atmospheric conditions at any point and at any time, is partly satisfied in the following restricted scenario; air density data was compared to *GOCE* measurements, at a height of 260 km - 290 km, within the 2010-2012 year range. Consequently, the following conclusions apply to the restricted analysis conditions.

The results delivered by *MET-07* and *DTM-2013* tended to overestimate actual data in noticeably higher percentages, being *MET-07* the one with lowest overall performance. Since the *MET-07* is a semi-empirical model, it could be due to its coefficients not being properly fitted and or the use of different satellite measurements on its parametrization that were not *GOCE*. As it is addressed in the following section, *Future Work*, it would be recommendable to extent the analysis to different parameters over longer periods and at different heights, which would lead to conclusions based on wider test scenarios.

It was concluded that the models of higher overall performance over the periods of different solar and geomagnetic activity studied are *JB-2008* and *NRLMSIS-00*. They provided results that tend to slightly overestimate actual *GOCE* density measurements, but succeeded to deliver results within a $\pm 5\%$ with respect to the latter. *JB-2008* performance was specially good in the period of low solar and moderate geomagnetic activity (period 1), which could be due to the use of the Dst

index for density changes during geomagnetic storms.

Furthermore, solar and geomagnetic activities have been realized to have a great effect on atmosphere dynamics, leading to the thermosphere "puff-up" phenomenon. It consists on higher layers being replaced by underneath denser layers when the thermosphere is heated, which causes the thermosphere to be denser at the same height. These effects are quite difficult to introduce in atmospheric models, usually by using the $F_{10.7}$ and Ap flux indices as proxies.

Also, positive socio-economic impact related to the development of accurate atmospheric models is realized, as they are crucial for atmospheric drag estimation.

7.2 Future Work

During the development of the present project, several ideas for future works have emerged in response to different needs that were not realized at the beginning of the investigation.

As an added key factor for the determination of the models for implementation, an study of the continuity of the density function would be useful for semi-analytic applications, since a continuous density function does not depend on altitude.

As it was mentioned before, being able to retrieve satellite measurements (i.e from satellite-borne accelerometers) is a struggle. It can be the case where a formal registration on the website that holds the data is needed, followed by an specific request for it, which leads to a waiting time for this request to be approved and finally to its downloading. In many cases, examples of how the data is presented and its format are not provided prior to its request, so it is quite possible that these data end up not being what you expected and/or needed. It is also quite common to follow several links on a website which are supposed to lead you to data download but this point is never reached, usually because the data is no longer available. The most common situation encountered was the downloading of data in binary code (raw data), which makes it hard to process by someone who is inexperienced. The difficulty in finding easy-to-use and accessible databases makes it hard to do research and it becomes unnecessarily time-consuming. Therefore, it would be considered helpful to develop an accessible and complete database, backed by the different organizations involved in this area, with the processed products of different satellite missions, which can be easily interpreted (including detailed explanation of what the data presents, units, etc) and having the same format to the extend possible. The community would have access to these public data stored in a same location; being a complete historical compilation of satellite-obtained data: temperature, density, composition, winds, magnetic field, etc. On the same line, as different atmospheric models use different solar and geomagnetic proxies as inputs, one historical database including registered actual and predicted values of these indices from different observatories would be useful. A complete set of $F_{10.7}$,

F_{30} values from which their means (monthly/smoothed) could be easily calculated, as well as k_p, A_p and a_P values, to name a few.

Satellites do not acquire acquire atmospheric conditions (density, temperature, etc) directly. These data is inferred from measurements taken using the different techniques explained in the paper. An interesting exercise would be to, for example, derive atmospheric density using satellite-borne accelerometer data. The more accurately these instruments are, the better the density values inferred represent reality, which can be then used for the parametrization of semi-empirical models.

Even tough programs written in C and FORTRAN are of higher computational power, it might be interesting to adapt the atmospheric models to be run by other programs. For example, *Dr. Paul Cefola* has expressed his interest in adapting the *GOST-2004* model to MATLAB, as *JB-2008* already is a MATLAB function within its directory. This could be useful for atmospheric modelling at a lower-skilled level, where accuracy is not as important, such as for academic purposes.

To complete the *a posteriori* analysis carried out in this project, data from satellites at different heights could be analyzed, for example from *CHAMP* and *GRACE* after being decoded, and implementing more models like the *GRAM*. The study could not only analyze air density, but more outputs like temperature and composition. Also, past solar cycles where solar activity was higher can be studied. Furthermore, an *a priori* analysis would be useful to see how well the models are able to estimate atmospheric conditions based on predicted values of solar and geomagnetic activity indices.

Extensive monitoring (not just observing) of the solar cycle can be considered as a quite new activity. It approximately started on 1996 with the 23^{rd} solar cycle since 1775. As predicting solar activity is the main source of uncertainty in the models and presents its largest error, it is important to keep monitoring it and trying to figure out the best way to introduce its effects in the models. For example, the inclusion of new space weather indices in the *JB-2008* is proof of the continued efforts of scientists who keep enhancing these models. It is clear that atmospheric modelling is not an easy task but essential for space applications, therefore, further and constant work on its development needs to prevail.

References

[1] Roger D. Launius. *Sputnik and the Origins of the Space Age*. NASA. URL: https://history.nasa.gov/sputnik/sputorig.html (visited on 07/21/2018).

[2] David Rising. *Satellite hits Atlantic — but what about next one?* The Oklahoman. Associated Press. Nov. 2013. URL: https://newsok.com/article/feed/615022/satellite-hits-atlantic-but-what-about-next-one (visited on 03/14/2018).

[3] ESA. *Building the International Space Station*. ESA. URL: http://www.esa.int/Our_Activities/Human_Spaceflight/International_Space_Station/Building_the_International_Space_Station3 (visited on 07/24/2018).

[4] *Sputnik 1*. NASA. Searched under Google Creative Commons filter. URL: https://nssdc.gsfc.nasa.gov/nmc/masterCatalog.do?sc=1957-001B (visited on 07/24/2018).

[5] *STS-132 undocking iss2*. Wikimedia. Searched under Google Creative Commons filter. URL: https://commons.wikimedia.org/wiki/File:STS132_undocking_iss2.jpg (visited on 07/24/2018).

[6] NASA. *Vostok 1*. NASA. Nov. 2013. URL: https://nssdc.gsfc.nasa.gov/nmc/spacecraftDisplay.do?id=1961-012A (visited on 07/24/2018).

[7] NASA. *NASA, Space Community Remember 'Freedom 7'*. NASA. May 2011. URL: https://www.nasa.gov/topics/history/features/50_freedom7.html (visited on 07/24/2018).

[8] NASA. *Space Shuttle Overview: Atlantis (OV-104)*. Kenney Space Center. 2013. URL: https://www.nasa.gov/centers/kennedy/shuttleoperations/orbiters/atlantis-info.html (visited on 07/25/2018).

[9] Bryan R. Swopes. *8 July 2011, 15:29:03 UTC, T minus Zero*. This Day in Aviation: Important Dates in Aviation History. 2016. URL: https://www.thisdayinaviation.com/tag/space-shuttle-atlantis-ov-104/ (visited on 07/26/2018).

[10] *Vostok Spacecraft*. Wikimedia. Searched under Google Creative Commons filter. URL: https://commons.wikimedia.org/wiki/File:Vostok_spacecraft.jpg (visited on 07/24/2018).

[11] *Mercury 3*. Wikimedia. Searched under Google Creative Commons filter. URL: https://commons.wikimedia.org/wiki/File:Mercury_3.jpg (visited on 07/24/2018).

[12] *STS-112 Atlantis carrying S1 struss*. Wikimedia. Searched under Google Creative Commons filter. URL: https://commons.wikimedia.org/wiki/File:STS-112_Atlantis_carrying_S1_truss.jpg (visited on 07/26/2018).

[13] Robert A. Braeunig. *Atmospheric models*. Rocket & Space Technology. 2014. URL: http://www.braeunig.us/space/atmmodel.htm (visited on 08/27/2018).

[14] William W. Vaughan. "Guide to Reference and Standard Atmospherics Models". In: *American Institute of Aeronautics and Astronautics (AIAA)* (2010), pp. 1–141.

[15] Committee on Space Research (COSPAR). *About COSPAR*. COSPAR. 2012. URL: https://cosparhq.cnes.fr/about (visited on 03/14/2018).

[16] NASA. *What is NASA?* NASA. 2008. URL: https://www.nasa.gov/audience/forstudents/5-8/features/nasa-knows/what-is-nasa-58.html (visited on 07/26/2018).

[17] NASA. *About Marshall*. NASA. 2017. URL: https://www.nasa.gov/centers/marshall/overview/about.html (visited on 07/27/2018).

[18] U.S Air Force. *Air Force Research Laboratory*. U.S Air Force. 2014. URL: http://www.af.mil/About-Us/Fact-Sheets/Display/Article/104463/air-force-research-laboratory/ (visited on 07/26/2018).

[19] Smithsonian Astrophysical Observatory. *SAO History*. CfA Harvard. URL: https://www.cfa.harvard.edu/about/aboutSAO (visited on 07/27/2018).

[20] US Air Force. *Air Force Space Command*. Air Force Space Command. 2018. URL: https://www.afspc.af.mil/About-Us/Fact-Sheets/Display/Article/249014/air-force-space-command/ (visited on 07/27/2018).

[21] CK-12 Foundation. *Importance of the Atmosphere*. CK-12. 2018. URL: https://www.ck12.org/earth-science/importance-of-the-atmosphere/lesson/Importance-of-the-Atmosphere-HS-ES/ (visited on 07/19/2018).

[22] NASA. *Energy: The Driver of Climate; Earth's atmosphere*. Climate Science Investigation (CSI). 2016. URL: http://www.ces.fau.edu/nasa/module-2/atmosphere/earth.php (visited on 07/19/2018).

[23] NASA. *Earth's Atmospheric Layers*. NASA. 2017. URL: https://www.nasa.gov/mission_pages/sunearth/science/atmosphere-layers2.html (visited on 07/19/2018).

[24] George Dvorsky. *Large Plasma Tubes Confirmed to Exist Above the Earth's Atmosphere*. iO9: We come from the Future. 2015. URL: https://io9.gizmodo.com/large-plasma-tubes-confirmed-to-exist-above-the-earths-1708434105 (visited on 08/01/2018).

[25] W. Priester, M. Roemer, and H. Volland. "The Physical Behaviour of the Upper Atmosphere deduced from Satellite Drag Data". In: *Space Science Reviews* 6 (2010), pp. 707–780.

[26] *03 Solar Wind*. Flickr. Searched under Google Creative Commons filter. Modified image. URL: https://www.flickr.com/photos/11304375@N07/2819711753/in/photostream/ (visited on 08/03/2018).

[27] NOAA: National Oceanic and Atmospheric Administration. *Where is space?* NESDIS News & Articles. 2016. URL: https://www.nesdis.noaa.gov/content/where-space (visited on 07/20/2018).

[28] *What are sunspots?* Space Weather Live. 2018. URL: https://www.spaceweatherlive.com/en/help/what-are-sunspots (visited on 08/28/2018).

[29] NASA. *What is the solar cycle?* NASA Space Place. Oct. 2017. URL: https://spaceplace.nasa.gov/solar-cycles/en/ (visited on 08/28/2018).

[30] *Sunspots 1302 Sep 2011 by NASA*. Wikimedia. Searched under Google Creative Commons filter. URL: https://commons.wikimedia.org/wiki/File:Sunspots_1302_Sep_2011_by_NASA.jpg (visited on 08/28/2018).

[31] Frank A. Marcos. "New Satellite Drag Modeling Capabilities". In: *American Institute of Aeronautics and Astronautics (AIAA)* (2006), pp. 1–13.

[32] *Solar Cycle Progression*. SpaceWeatherLive. Modified image. URL: https://www.spaceweatherlive.com/en/solar-activity/solar-cycle (visited on 08/22/2018).

[33] Travis Francis Lechtenberg. *Density model corrections derived from orbit data to characterize upper atmosphere density variations*. End of Degree Project, University of kansas.

[34] *The Ap Index*. Space Weather Live. 2018. URL: https://www.spaceweatherlive.com/en/help/the-ap-index (visited on 09/16/2018).

[35] National Centers for Environmental Information. *Geomagnetic Kp and Ap Indices*. NASA. URL: https://www.ngdc.noaa.gov/stp/geomag/kp_ap.html (visited on 08/08/2018).

[36] J.M Picone, A.E Hedin, and D.P. Drob. "NRLMSISE-00 Empirical Model of the Atmosphere: Statistical Comparisons and Scientific Issued". In: *Journal of Geophysical Research* (2002).

[37] National Oceanic Space Weather Prediction Center and Atmospheric Administration. *Satellite Drag*. SPWPC, NOAA. URL: https://www.swpc.noaa.gov/impacts/satellite-drag (visited on 08/01/2018).

[38] NASA GSFC Atmospheric Experiments Laboratory. *Huygens Probe, Gas Chromatograph Mass Spectrometer*. NASA. URL: https://attic.gsfc.nasa.gov/huygensgcms/Mass_Spec_Intro.htm (visited on 08/04/2018).

[39] PREMIER Biosoft. *Mass Spectrometry*. PREMIER Biosoft: Accelerating Research in Life Sciences. URL: http://www.premierbiosoft.com/tech_notes/mass-spectrometry.html (visited on 08/04/2018).

[40] Dr. Volker Grassmann. *Incoherent Scatter: Principles and Applications*. DF5AI. URL: http://df5ai.net/ArticlesDL/IScatter(E).pdf (visited on 08/05/2018).

[41] M.P Sulzer. "RADAR: Incoherent Scatter Radar". In: *Encyclopedia of Atmospheric Sciences* 2 (2015), pp. 422–428.

[42] *Millstone Hill Radar - Haystack Observatory - DSC04019*. Wikimedia. Searched under Google Creative Commons filter. URL: https://commons.wikimedia.org/wiki/File:Millstone_Hill_Radar_-_Haystack_Observatory_-_DSC04019.JPG (visited on 08/05/2018).

[43] NASA Space Vehicle Design Criteria (Guidance and Control). *Space Vehicle Accelerometer Applications*. NASA. 1972. URL: https://ntrs.nasa.gov/archive/nasa/casi.ntrs.nasa.gov/19730018164.pdf (visited on 08/06/2018).

[44] NASA's Earth Observing System. *Challenging Mini-satellite Payload (CHAMP)*. NASA. URL: https://eospso.nasa.gov/missions/challenging-mini-satellite-payload (visited on 08/07/2018).

[45] Touboul E. et al. "Accelerometers for CHAMP, GRACE and GOCE space missions: synergy and evolution". In: *Bolletino di Geofisica Teorica ed Applicata* 40 (1999), pp. 321–327.

[46] Bruinsma S., Tamagnan D., and Biancle R. "Atmospheric densities derived from CHAMP/STAR accelerometer observations". In: *Planetary and Space Science* 52 (2004), pp. 297–312.

[47] *CHAMP-concept*. Wikimedia. Searched under Google Creative Commons filter. URL: https://commons.wikimedia.org/wiki/File:CHAMP_concept.png (visited on 08/07/2018).

[48] *Earth Global Reference Atmospheric Model 2010 (Earth GRAM 2010)*. NASA Software. URL: https://software.nasa.gov/software/MFS-32780-1 (visited on 09/14/2018).

[49] *NRLMISIS-OO Atmosphere Model*. Community Coordinated Modeling Center. URL: https://ccmc.gsfc.nasa.gov/modelweb/models/nrlmsise00.php (visited on 09/14/2018).

[50] *The Jacchia-Bowman 2008 Empirical Thermospheric Density Model*. Apr. 2015. URL: http://sol.spacenvironment.net/jb2008/index.html (visited on 09/14/2018).

[51] *Model*. ATMOP: Advanced Thermosphere Modelling for Orbit Prediction. URL: http://www.atmop.eu/index.php/component/dtm/?Itemid=692 (visited on 09/14/2018).

[52] *Jacchia-Bowman Atmospheric Density Model*. Mathworks. Apr. 2015. URL: https://es.mathworks.com/matlabcentral/fileexchange/56163-jacchia-bowman-atmospheric-density-model?s_tid=srchtitle (visited on 09/14/2018).

[53] *What is Universal Time?* Time and Date. URL: https://www.timeanddate.com/time/universal-time.html (visited on 08/08/2018).

[54] Columbia University. *Solar Time*. Infoplease. 2012. URL: https://www.infoplease.com/encyclopedia/science-and-technology/astronomy-and-space-exploration/astronomy-general/solar-time (visited on 08/08/2018).

[55] K. F. Tapping. "The 10.7 cm solar radio flux ($F_{10.7}$". In: *Space Weather* 11 (2013), pp. 394–406.

[56] SWPC. *Space Weather Prediction Center: Report of Solar and Geophysical Activity*. NASA Space Place. Jan. 2008. URL: http://legacy-www.swpc.noaa.gov/ftpdir/forecasts/RSGA/README (visited on 08/29/2018).

[57] *RSGA warehouse*. SWPC, NOAA. URL: ftp://ftp.swpc.noaa.gov/pub/warehouse/ (visited on 09/14/2018).

[58] Center for Space Standards & Innovation. *EOP and Space Weather Data*. CelesTark. Sept. 2008. URL: http://www.celestrak.com/SpaceData/ (visited on 09/17/2018).

[59] NASA Goddard Space Flight Center: Space Physics Data Facility. NASA ATMOWEB. URL: https://omniweb.gsfc.nasa.gov/ftpbrowser/atmoweb.html (visited on 09/14/2018).

[60] ESA. *GOCE*. ESA. URL: http://m.esa.int/Our_Activities/Operations/GOCE (visited on 09/07/2018).

[61] *GOCE+ Thermospheric Data*. ESA GOCE Virtual Archive. URL: http://eo-virtual-archive1.esa.int/GOCE-Thermosphere.html (visited on 09/14/2018).

[62] *SWARM (Geomagnetic LEO Constellation*. eoPortal Directory. URL: http://m.esa.int/Our_Activities/Operations/GOCE (visited on 09/07/2018).

[63] *SWARM DATA ACCESS*. ESA. URL: https://swarm-diss.eo.esa.int/# (visited on 09/14/2018).

[64] PDGS Team. *Swarm Users - Data Access Manual*. English. ESA. 20 pp. June 21, 2018.

[65] GFZ Helmholtz Centre Postdam. Information Systems and Data Center. URL: http://isdc-old.gfz-potsdam.de/index.php (visited on 09/14/2018).

[66] *Solar cycles 21-24*. Solen info. URL: http://www.solen.info/solar/solcycle_old.html (visited on 09/03/2018).

[67] Sean Bruinsma. *The contribution of GOCE densities to the semi-empirical thermosphere model DTM*. 5th GOCE user workshop. (Visited on 09/25/2018).

[68] Gary Brown and William Harris. *How Much Do SAtellites Cost?* URL: https://science.howstuffworks.com/satellite10.htm (visited on 09/18/2018).

[69] Xavier Fontdegloria. "La estación espacial china". In: *El País* (2018).

Appendix A

List of abbreviations

Acronym	Stands for
AE	Atmospheric Explorer
AFGL	Air Force Geophysics Laboratory
AFRL	Air Force Research Laboratory
AIAA	American Institute of Aeronautics and Astronautics
ATMOP	Advanced Thermosphere Modeling of Orbit Prediction
CCMC	Community Coordinated Modeling Center
CHAMP	Challenging Micro-satellite Payload
CIRA	COSPAR International Reference Atmosphere
COSPAR	Committee on Space Research
CNS	Centre National d'Estudes Spatiales
CSA	Canadian Space Agency
CSSI	Center for Space Standards & Innovation
DCA	Dynamic Calibration Atmosphere
EISCAT	European Incoherent Scatter Scientific Association
EOP	Earth Orientation Parameter
ESA	European Space Agency
EUMETSAT	European Organization for the Exploitation of Meteorological Satellites
GOCE	Gravity Field and steady-state Ocean Circulation Explorer
GOST	Russian Earth's Upper Atmosphere Density Model Satellites for Ballistic Support of the Flight of Artificial Earth
GPS	Global Positioning System
GRACE	Gravity Recovery and Climate Experiment

Acronym	Stands for
GRAM	Global Reference Atmospheric Model
GSO	Geosynchronous Orbit
HASDM	High Accuracy Satellite Drag Model
ICSU	International Council of Scientific Unions
IR	Infrared Radiation
IRS	Incoherent Scatter Radar
ISDC	Information System and Data Center
ISS	International Space Station
ISO	International Organization for Standardization
JAXA	Japan Aerospace Exploration Agency
JB	Jacchia-Bowman
LEO	Low Earth Orbit
LST	Local solar time
MET	Marshall Engineering Thermosphere Model
MetOp	Meteorological Operational satellite
MEO	Medium Earth Orbit
MSFC	Marshall Space Flight Center
MSIS	Mass Spectrometer-Incoherent Scatter
MSISE	Mass Spectrometer and Incoherent Scatter Radar Extended
NASA	National Aeronautics and Space Administration
NGA	National Geospatial-intelligence Agency
NOAA	National Oceanic and Atmospheric Administration
NRL	Naval Research Laboratory
RSGA	Report of Solar and Geophysical Activity
SAG	SHARC Atmosphere Generator

Acronym	Stands for
SAMM	SHARC and MODTRAM Merged
SHARC	Strategic High-Altitude Radiance Code
SLR	Satellite Laser Ranging
SWPC	Space Weather Prediction Weather
STAR	Space Three-Axis Accelerometer for Research
URSI	International Union of Radio Science
US	United States
USSR	Union of Soviet Socialist Republics
UT	Universal Time